

Review

Advancements and Applications of Redox Flow Batteries in Australia

Touma B. Issa , Jonovan Van Yken, Pritam Singh  and Aleksandar N. Nikoloski * 

Harry Butler Institute (Centre for Water Energy and Waste), School of Engineering & Information Technology, Murdoch University, Perth, WA 6150, Australia; t.issa@murdoch.edu.au (T.B.I.);
jonovan.vanyken@murdoch.edu.au (J.V.Y.); p.singh@murdoch.edu.au (P.S.)

* Correspondence: a.nikoloski@murdoch.edu.au

Abstract: Redox flow batteries (RFBs) are known for their exceptional attributes, including remarkable energy efficiency of up to 80%, an extended lifespan, safe operation, low environmental contamination concerns, sustainable recyclability, and easy scalability. One of their standout characteristics is the separation of electrolytes into two distinct tanks, isolating them from the electrochemical stack. This unique design allows for the separate design of energy capacity and power, offering a significantly higher level of adaptability and modularity compared to traditional technologies like lithium batteries. RFBs are also an improved technology for storing renewable energy in small or remote communities, benefiting from larger storage capacity, lower maintenance requirements, longer life, and more flexibility in scaling the battery system. However, flow batteries also have disadvantages compared to other energy storage technologies, including a lower energy density and the potential use of expensive or scarce materials. Despite these limitations, the potential benefits of flow batteries in terms of scalability, long cycle life, and cost effectiveness make them a key strategic technology for progressing to net zero. Specifically, in Australia, RFBs are good candidates for storing the increasingly large amount of energy generated from green sources such as photovoltaic panels and wind turbines. Additionally, the geographical distribution of the population around Australia makes large central energy storage economically and logically difficult, but RFBs can offer a more locally tailored approach to overcome this. This review examines the status of RFBs and the viability of this technology for use in Australia.



Academic Editor: David Zitoun

Received: 6 January 2025

Revised: 5 February 2025

Accepted: 14 February 2025

Published: 16 February 2025

Citation: Issa, T.B.; Van Yken, J.; Singh, P.; Nikoloski, A.N.

Advancements and Applications of Redox Flow Batteries in Australia.

Batteries **2025**, *11*, 78. <https://doi.org/10.3390/batteries11020078>

Copyright: © 2025 by the authors. Licensee MDPI, Basel, Switzerland. This article is an open access article distributed under the terms and conditions of the Creative Commons Attribution (CC BY) license (<https://creativecommons.org/licenses/by/4.0/>).

1. Introduction

Currently, society is facing an environmental and energy crisis [1–3]. There are many factors that are contributing to this, including the use of fossil fuels as a source of energy [4,5]. Burning fossil fuels, such as coal, oil, and natural gas, to produce energy causes air and water pollution. Fossil fuels generate a large amount of greenhouse gas (GHG) emissions, such as carbon dioxide (CO₂) [3,6,7], methane (CH₄), and nitrous oxide (N₂O) which, in addition to chlorofluorocarbons (CFC) and water vapour, form the five key greenhouse gases [8,9]. Their presence traps the sun's heat in the earth's atmosphere and slows down heat loss to space.

To meet increases in energy demand while reducing GHG emissions associated with electricity generation, the world needs to transition to more environmentally friendly energy sources [3,10]. This transition should be as smooth as possible to ensure minimal

disruptions to industry and the global economy, as well as maintaining or improving standards of living.

Renewable energy sources such as wind and solar have been utilised as alternatives to fossil fuel-based energy sources and are increasingly being integrated into the global energy resource [3,11,12], which is helping to reduce the dependency on fossil fuels as the primary source of energy. In 2023, wind, solar, and other renewables, including hydro-based-energy sources, accounted for 36% of total energy supply globally [13,14]. The transition to renewable energy generation is expected to accelerate significantly in the coming years, with wind and solar increases from 2018 to 2050 predicted to be 14-fold and 30-fold, respectively [13]. Australia is rapidly adapting to renewable energy and currently has the largest residential photovoltaic (PV) system uptake globally, with 21% of residential homes having rooftop PV panels [15].

A notable drawback of this technology, however, is that renewable energy sources are irregular in energy generation, and there is therefore a need for reliable energy storage systems (ESSs) or electrical energy storage systems (EESs) with high safety and low cost. ESSs (or EESs) are a method of converting electrical energy from a power generating system into a form that can be stored then converted back to electrical energy when required. ESSs store the excess energy generated from renewable sources when it is in surplus and feed it back into the power grid when needed, such as during peak hours or when no energy is being generated [3,16,17]. ESSs should be regarded as essential infrastructure for the energy transition. A variety of different types of ESSs are available with the selection of a specific type depending on location, demand, capacity, and costs of investment (Figure 1).

The number of photovoltaic panels currently installed in Australian households is very large. However, despite the large amount of electrical energy generated by residential PV systems, these systems can be a threat to the stability of the overall electricity grid and when the energy provided to the grid by these resources surpasses 10–20% of the overall energy production [18,19]. In recent years, solar farms have been required to shut down when there is an oversupply of energy [20,21]. A substantial network of distributed energy storage systems could solve many of these issues with Australia’s current renewable energy system. In addition, energy storage systems are essential where there is night-time use of electricity in houses, health and aged care facilities, and any business with night-time operations that only gets its electricity from solar PV [3].

There are several technologies (Figure 1) that store electrical energy and can later return it to the grid. These energy storage systems are classified as electrochemical (batteries and supercapacitors), chemical, electrical (capacitors and superconducting magnets), thermal, and mechanical (pumped hydropower (PHS), fly wheel, and compressed air) [22].

Every energy storage system has challenges, but batteries, in general, which are electrochemical storage systems, are the most developed and flexible form of energy storage [23]. Even though PHS is considered, in certain circumstances, the most developed electricity storage technology, its utilisation is very limited [24]. Batteries are very fast to respond to demands for power not met by renewable energy generation, and they provide stability when integrated into the main electricity grid better than other energy storage systems. The calculated return on capital investments for batteries may be ten years or more [25], but this may reduce in the future as the cost of battery components reduces.

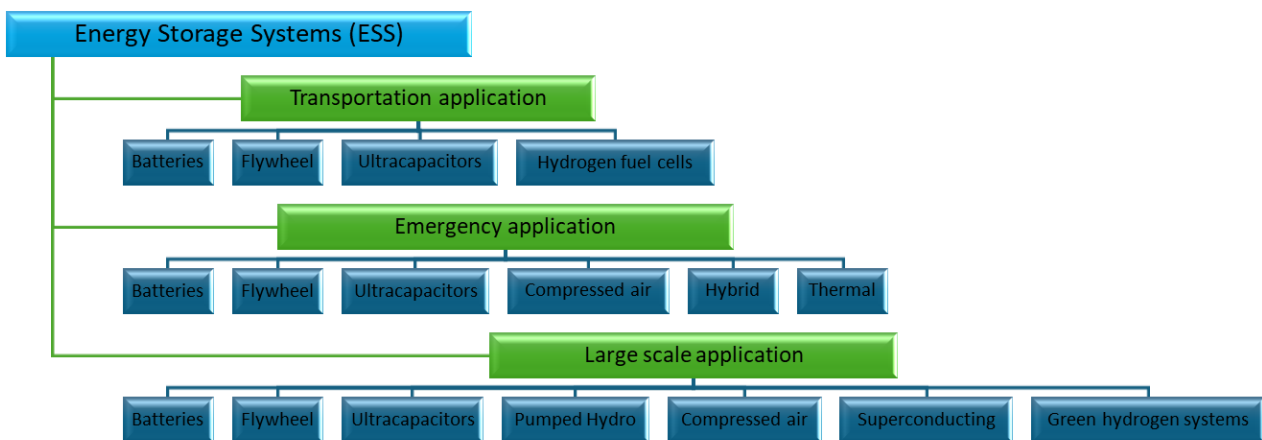


Figure 1. Classification of the principal energy storage systems (adapted from [26]).

An increasing demand for ways to store the energy produced from renewables has led to a rapid advancement in battery technology. Flow batteries are considered promising in the large-scale commercial and grid-scale storage markets [3,27–29]. The recent installation of redox flow batteries (RFBs) alongside solar PV by Yadlamalka Energy [30–32], a first of its kind in Australia, is an excellent example of use of this technology. Australian company, Thorion energy, partnered with SMEC Power and Technology to trial the use of its redox flow batteries at mine sites in Western Australia in 2023 [33]. Capital cost analysis indicates that RFBs are cost-effective for long discharge duration applications [34] and have long cycle lives [35], making them an excellent choice for large-scale or remote energy storage. Recently, a 78 kW/220 kWh vanadium redox flow battery was deployed by Horizon Power in Kununurra, Western Australia. This battery, manufactured by Invinity Energy Systems, was supplied and commissioned by VSUN Energy [36].

2. Redox Flow Batteries (RFBs)

2.1. Basic Construction

The origins of the concept underlying redox flow batteries (RFBs) can arguably be traced to 1884 with Renard's chlorine-chromium battery, developed for "La France" airship propulsion. However, this device was a primary cell and did not utilise electrolyte flow [37], distinguishing it from the modern RFB architecture. A process for storing electrical energy in liquids was patented as early as 1949 by Walther Kangro [3,38,39]. Several groups worldwide are currently working on the development of RFBs. Full-scale development of RFBs started in the 1970s. The principle of the RFB system was presented by L. H. Thaller in 1974 based on research conducted at the National Aeronautics and Space Administration (NASA) and focusing on the iron chromium (Fe/Cr) system [40]. The word "Redox" is an abbreviation of reduction and oxidation and describes the reactions that occur in these batteries. RFB liquid electrolytes contain electroactive redox species dissolved or suspended in a supporting electrolyte which is used to increase conductivity. The electrolyte is always kept in two separate tanks and is propelled through the electrochemical cell or the battery stack using pumps. A cooling system is also needed as charge and discharge of RFBs involves heat release [3]. Oxidation and reduction reactions between the two electroactive species occur on the surface of electrodes, where the electrical energy is converted to chemical energy during charge and vice versa during discharge (Figure 2) [3].

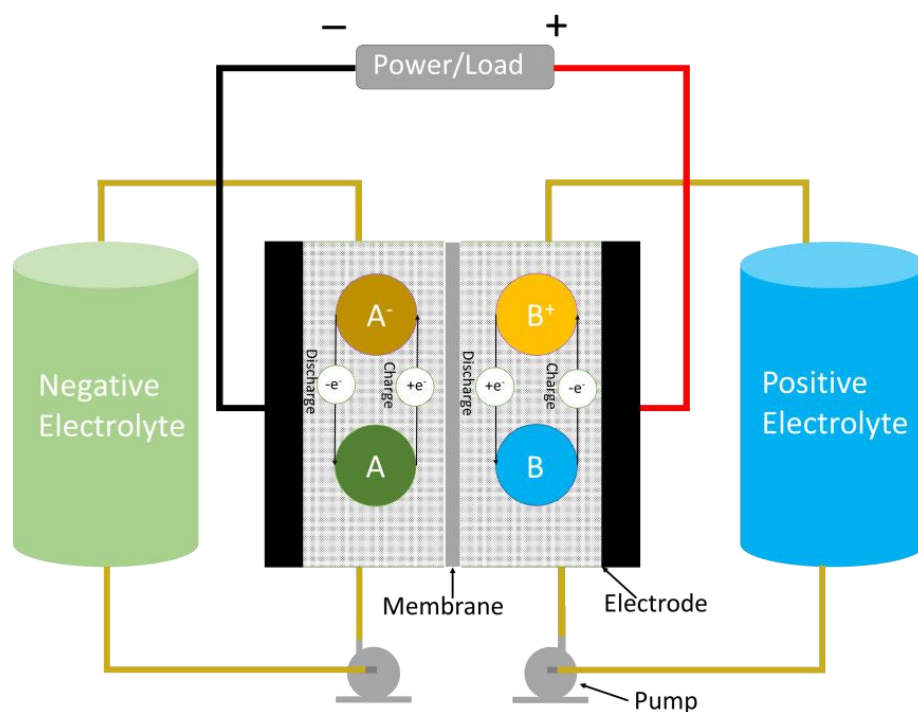


Figure 2. General schematic of RFB operation. Redox reactions take place inside the cell (marked with a blue dashed rectangle) on the surface of the electrodes (black rectangles). The electrolyte is continuously renewed by pumping solution from the tanks. The direction of electron flow (charge or discharge) is managed by the electrical components, which either act as a power source or load the energy from the battery.

During charging the battery stores energy in the liquid electrolyte that flows through a stack of electrochemical cells. In the charge part of the cycle, an electron is liberated through an oxidation reaction from a high chemical potential state on the negative or anode side of the cell stacks. This electron reaches the positive or cathode side through an external connection (usually an electric wire) and is accepted through a reduction reaction at a lower chemical potential state, allowing the storage of energy [3]. Ions cross from one side of the cell to the other side through a membrane to complete the circuit. For every electron transferred from the anolyte to the catholyte, a positive charge moves across the membrane to maintain electroneutrality. The reverse process happens in the discharge cycle [3].

In practice, a flow battery system has a distinctive configuration (Figure 3). The structure of a typical RFB contains carbon felt or carbon plastic electrodes, bipolar plates usually made from graphite (these prevent direct contact between the electrolyte and current collectors), membranes (that may be an anionic exchange membrane, or a cationic exchange membrane) or a separator, a flow frame (to direct the electrolyte flow through the electrodes), and an end plate with electrolyte fittings and current collector. This is the working unit of an RFB and is separated from the bulk of the electrolyte. As such, it can be modified to suit the needs of the system independently from the electrolyte storage system [41]. For larger operations, the cells are stacked together.

The electrolyte flows from each electrolyte storage tank through the cell stack and back to that electrolyte storage tank. The energy conversions from electrical energy to chemical potential (for charging) and vice versa (for discharging) take place rapidly at the surface of the electrodes as soon as the liquid electrolytes flowing through each cell flow past one another in the stack [3].

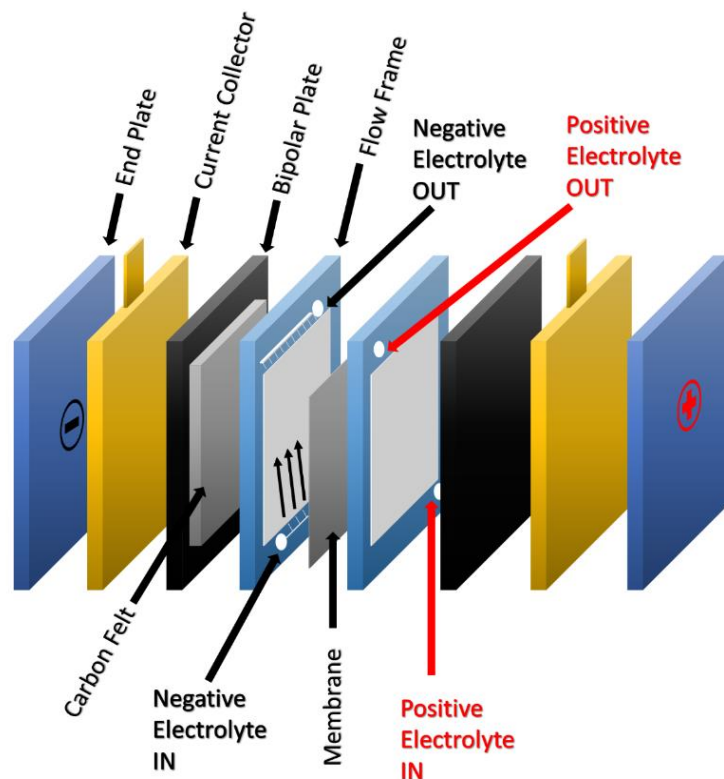


Figure 3. Illustration of the structure of a redox flow battery cell showing the most important components. Flow is indicated by the arrows in the flow frame.

The flow is provided via a series of pumps which in turn are controlled by a central control system. The system is connected to the grid through an inverter [41], completing the integrated battery storage system (Figure 4).

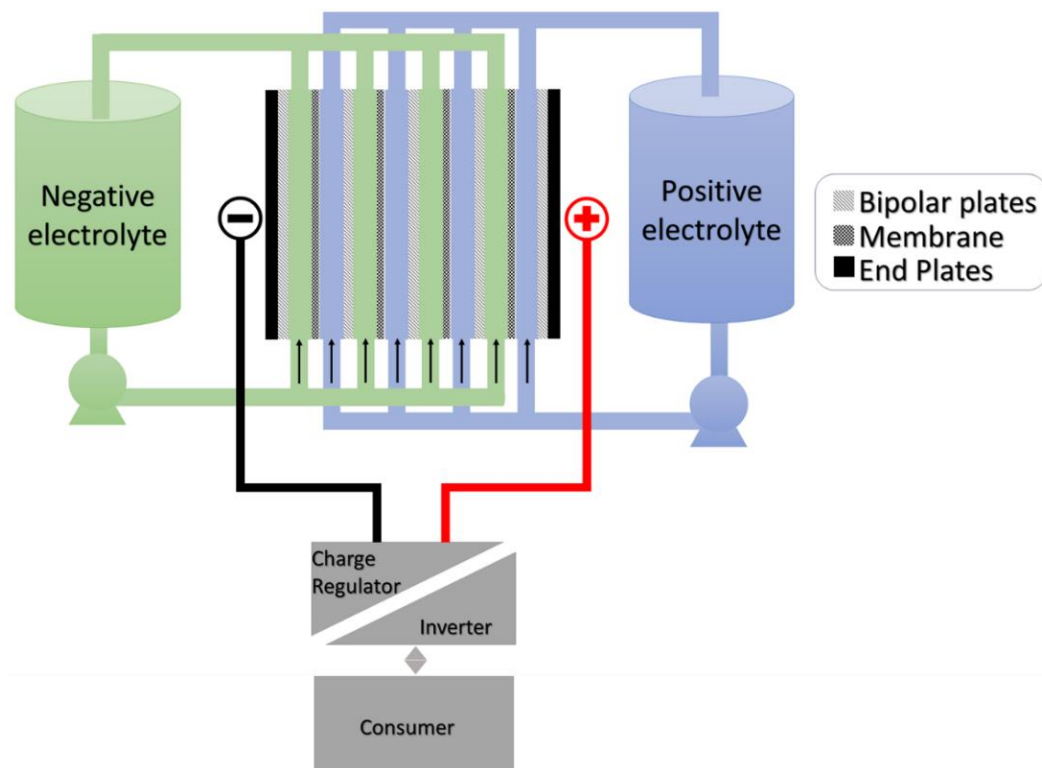


Figure 4. A schematic diagram of the redox flow battery with four cells stack.

Due to the design of RFBs, the power (kW) and energy storage capacity (kWh) can be designed separately. While the size of the tanks (the volume of the electrolyte) controls the energy capacity of an RFB, the size of the electrodes and the number of cells (total surface area of all the cells) control the power of the battery [3].

A bipolar electrode design can be used to increase the specific energy of the battery. This design allows the current to travel directly through the battery stack since the electrochemical reactions take place on opposite sides of the bipolar electrodes. Unlike the encased configuration of a lithium-ion battery where energy is stored in rolled electrode sheets, a flow battery utilises electroactive species that are dissolved and freely migrate in liquid electrolytes and that are present in different oxidation states [3].

RFBs can be divided into classical or true RFBs and hybrid RFBs, which are further divided into Type I and Type II [42] (Figure 5). Classical RFBs use inert electrodes and redox species that remain in the solution. Examples of classical RFBs are the iron chromium (Fe/Cr) system [40], the bromine–polysulphide system [43,44], and the vanadium RFBs [45]. Hybrid RFB operation involves a phase change during the cell reaction. An example is the zinc/bromine system in which the plating and dissolution of zinc at the anode occur upon charge and discharge, respectively [46–51].

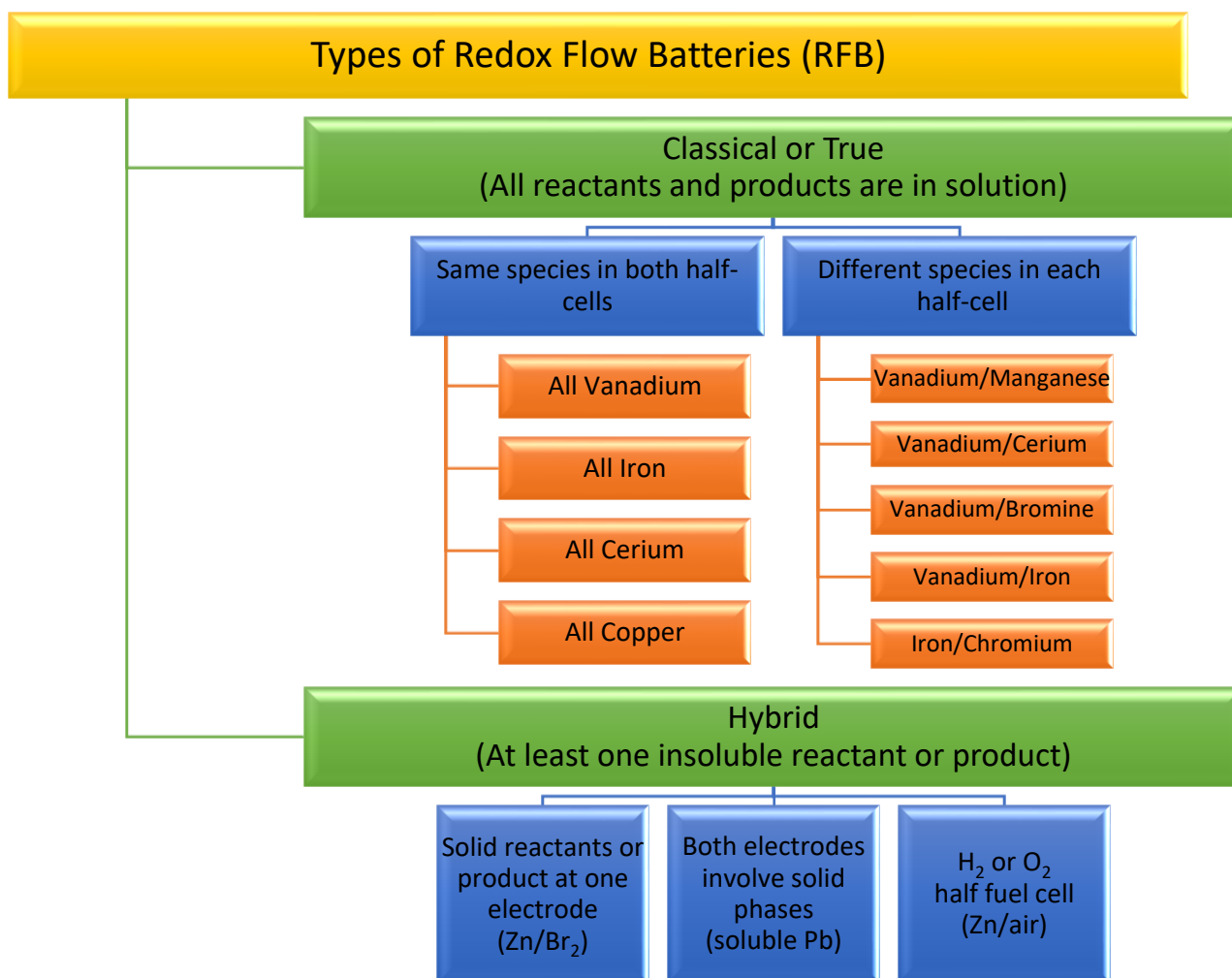


Figure 5. Classification of redox flow batteries, showing classical (redox/redox) and hybrid (solid layer/redox or gas/redox) types (adapted from [52]).

RFBs are well known for their long cycle life, modular design, excellent electrochemical reversibility, high round-trip efficiency, good scalability and flexibility, safety, indepen-

dent sizing of power and energy, deep discharge ability, short response time, moderate maintenance cost, and low environmental impact [3,53]. With these characteristics, RFBs can be used in applications with a range of operational power and discharge time requirements and are also suitable for supporting electricity generation from a range of renewable sources (Figure 6).

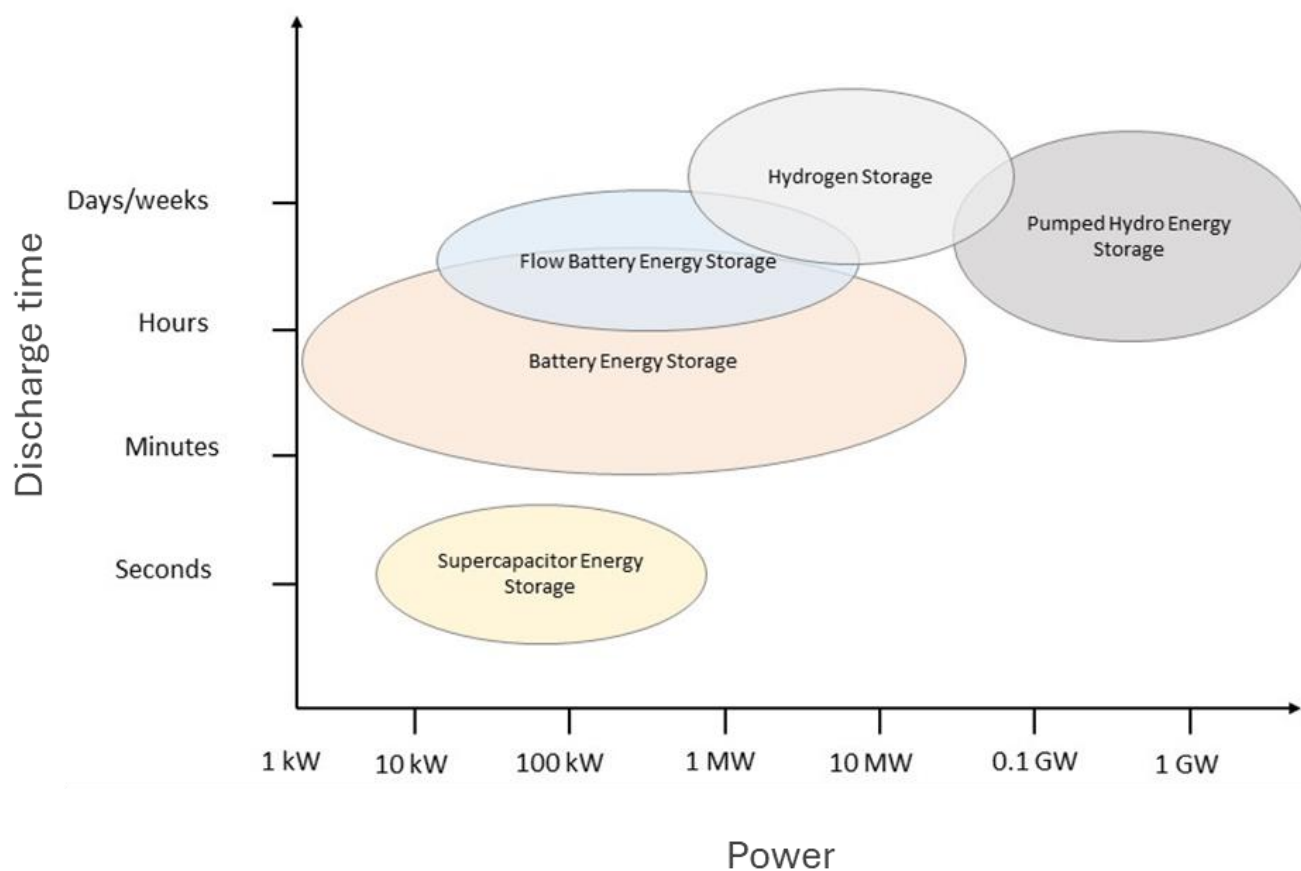


Figure 6. Diagram comparing power rating and discharge time of some energy storage systems (adapted from [54,55]).

RFBs can be easily integrated into applications that need energy storage systems for load-levelling, flex ramping, peak shaving, time shifting, maintaining power quality, and frequency regulation [41,56–58].

2.2. Redox Flow Battery Chemistry

Several combinations (more than 30) of redox pairs have been detailed in the literature as possible RFB electrolytes that contain two redox couples. Previous work summarised these combinations (Table 1) using data from published articles and/or patents [59]. Only five of these electrolytes are used in RFBs that are produced commercially: all-vanadium (V^{3+}/V^{2+} couple and V^{5+}/V^{4+} couple), iron chromium (Fe/Cr), zinc bromine (Zn/Br_2), all-iron (Fe^{2+}/Fe^{3+} couple and Fe^{2+}/Fe^0 couple), and polysulphide bromine (S_2/Br_2) systems. Most RFB electrolytes are acidic because many metal ions (except for zinc) precipitate as insoluble hydroxides at high pH values, and the alkaline electrolytes are therefore unsuitable [3]. Table 2 summarises electrical properties of redox flow batteries with different chemistries and Table 3 details the names, locations, and RFB system types of some flow battery companies.

Table 2. Electronic properties of selected redox flow batteries with different chemistries.

System	Open Circuit Potential (OCP) (V)	Current Density (mA/cm ²)	Charge/Discharge Efficiency (%)	Reference
Fe-Cr	1.18	21.5	95 (Coulombic)	[53,60]
Fe-Ti	1.19	14	44–50 (Overall)	[53]
VRB	1.6	10–130	80 (Overall)	[53]
V-Br	1.4	20	74 (Overall)	[61–66]
V-Fe				[34,67–69]
V-Mn	1.66	20	63 (Overall)	[70–72]
V-Ce	1.5	22	90 (Coulombic)	[73–79]
V-glyoxal (O ₂)	1.2	20	66 (Coulombic)	[53]
V-polyhalide	1.3	20	83 (Coulombic) 80 (Voltaic)	[53]
Hybrid V-O ₂ fuel cell	-	2.4	45.7 (Overall)	[53]
Zn-Br	1.85	20	80 (Overall)	[46–51,53,61,62,80–85]
Flow-through lead battery	1.62	20	60–66 (Overall)	[86]

Table 3. Examples of flow battery companies with RFB system types [87].

Company Name	Location	System
Australian Flow Batteries	Western Australia, Australia	VRFB
AVESS Energy	Western Australia, Australia	VRFB
CellCube (Enerox GmbH)	Wiener Neudorf, Austria	VRFB
ESS Tech Inc.	Wilsonville, Oregon, U.S.A.	Fe Flow
Invinity Energy Systems	St. Helier, Jersey	VRFB
Largo Inc.	Toronto, Ontario, Canada	VRFB
Lockheed Martin Corp.	Bethesda, Maryland, U.S.A.	Synthetic metal-ligand
Primus Power Solutions	Hayward, California, U.S.A.	Zn/Br ₂
Rongke Power	Dalian, China	VRFB
Redflow Technologies Ltd.	Queensland, Australia	Zn/Br ₂ (entered voluntary administration)
SCHMID Group	Freudenstadt, Germany	VRFB
Sumitomo Electric Ind., Ltd.	Osaka, Japan	VRFB
Thorion Energy	Perth, Western Australia, Australia	VRFB
Vecco Group	Queensland, Australia	VRFB
VRB Energy	Vancouver, British Columbia, Canada	VRFB
VisBlue	Denmark	VRFB
VFlow Tech	Singapore	VRFB
VSUN Energy	Western Australia, Australia	VRFB

2.3. Energy Efficiency

The system efficiency parameters for all batteries including RFBs are Coulombic efficiency, voltaic efficiency, and energy efficiency.

The Coulombic efficiency, CE, is the ratio of the amount of charge transferred upon the discharge ($Q_{\text{discharge}}$) to the amount of charge transferred upon the charge (Q_{Charge}). Coulombic losses are caused by several phenomena such as ion diffusion processes, irreversible reactions, and shunt currents through the electrolyte [88]. It is the purpose of the ion exchange membrane to prevent ion diffusion, and significant research has been conducted in membrane modification to ensure high selectivity without compromising performance [3,89–95].

$$CE = \frac{Q_{\text{discharge}}}{Q_{\text{Charge}}} \times 100\% = \frac{\int |i_{\text{discharge}}(t)| dt}{\int i_{\text{charge}}(t) dt} \times 100\% \quad (1)$$

The voltaic efficiency, VE, is the ratio of the average discharge voltage ($\bar{V}_{\text{discharge}}$) to the average charge voltage (\bar{V}_{charge}). VE losses occur when the average charging voltage is

consistently higher than the voltage required to activate the response of the material inside the battery. Another factor that reduces VE is the internal resistance of the battery, which increases with battery size, battery age, and current, and can be dependent on the battery chemistry [3].

$$VE = \frac{\bar{V}_{\text{discharge}}}{\bar{V}_{\text{charge}}} \times 100\% \quad (2)$$

The energy efficiency, EE, is calculated as the product of the Coulombic efficiency and the voltaic efficiency. The EE indicates how much of the energy that is supplied to the battery during charging can be extracted upon discharge [3].

$$EE = \frac{\int |i_{\text{discharge}}(t)| dt}{\int i_{\text{charge}}(t) dt} \times \frac{\bar{V}_{\text{discharge}}}{\bar{V}_{\text{charge}}} \times 100\% = CE \times VE \quad (3)$$

It should be noted, however, that the total system energy efficiency will be different in application. There is a net energy consumption from operating the pumps for each half-cell in a RFB as well as energy loss from flowing through pipes. This can be calculated using Equations (4) and (5) [96].

$$P_{NE} = P_{NE}^{\text{pipes}} + P_{NE}^{\text{pumps}} \quad (4)$$

$$P_{PE} = P_{PE}^{\text{pipes}} + P_{PE}^{\text{pumps}} \quad (5)$$

where P_{NE} is the net energy lost in the negative half-cell from the pipes (P_{NE}^{pipes}) and the energy consumed by the pumps (P_{NE}^{pumps}). Equation (5) calculates the same for the positive electrolyte (P_{PE}). The energy efficiency calculation (3) can be amended to account for this using Equation (6) [96].

$$EE_{\text{net}} = \frac{\int_0^{t_d} (E_{\text{discharge}} I_{\text{discharge}} - (P_{NE} + P_{PE}) dt)}{\int_0^{t_c} (E_{\text{charge}} I_{\text{charge}} + (P_{NE} + P_{PE}) dt)} \quad (6)$$

where EE_{net} is the net energy efficiency of the system, t_d is the discharging time, and t_c is the charging time. Note that the power provided to the load in the discharging process has been subtracted from the power wasted during the flow of the electrolytes in the pipe and expended by the pumps. In application, the total power required is the sum of the power expended by the pumps and pipes as well as that required by the chemical reaction.

3. Classical RFBs

3.1. All-Vanadium RFBs

The RFB type that has received the most attention is the all-vanadium redox flow battery (VRFB). VRFBs are considered to be one of the most promising grid-scale energy storage systems and are well suited for integration with renewable energy generation sources. This is due to their robustness under a wide range of operating conditions, the ability to set power and energy ratings independently, long maximum discharge and storage times, and safety, including non-flammability [3,97].

The vanadium (V) redox couple was first mentioned in a 1933 patent by P.A. Pisoort [98] and was suggested for use in batteries by NASA and by Pellegrini and Spaziente in 1978 [99]. The first known successful demonstration and patenting of VRFBs was carried out in Australia by Skyllas-Kazacos and co-workers at the University of New South Wales (UNSW) who registered a patent in 1988 [100]. Australia is ideally placed to produce VRFBs as vanadium resources are abundant. VRFBs have already proven their value, but several research groups around the world are looking to improve their performance and efficiency to achieve higher power outputs [3,101].

A VRFB power cell consists of two half-cells, with each half-cell consisting of an end plate, an end gasket, a bipolar plate (extruded sheet of carbon polymer material), a porous electrode (usually carbon felt), and a frame gasket. The two halves are separated by a membrane which is usually an ion exchange membrane (that may be an anionic exchange membrane or a cationic exchange membrane) [102] or a separator [103] (Figure 3). Electrical connection to the cells is normally achieved via a metal current collector (usually copper sheet or mesh) isolated from the battery electrolyte. A VRFB stack is made up of an assembly of these power cells [3].

The VRFB uses vanadium's capacity to exist in four different oxidation states [104] to create a battery with one electroactive element rather than two. By using vanadium redox couples in both half-cells, the issue of cross-contamination with another element caused by ion diffusion across the membrane is eliminated.

The electrochemical reactions occur on the inert carbon felt electrodes in the half-cells. Pipes and pumps are used to move the electrolyte from its storage tanks to the stack. As such, the correct pretreatment of these electrodes to ensure hydrophilicity and reduce faradaic resistance is important. The performance of a VRFB is not significantly degraded by repeated full discharge or charge rates as high as the maximum discharge rate, according to Skyllas-Kazacos and colleagues [105]. A schematic showing the reactions in a VRFB can be seen in Figure 7.

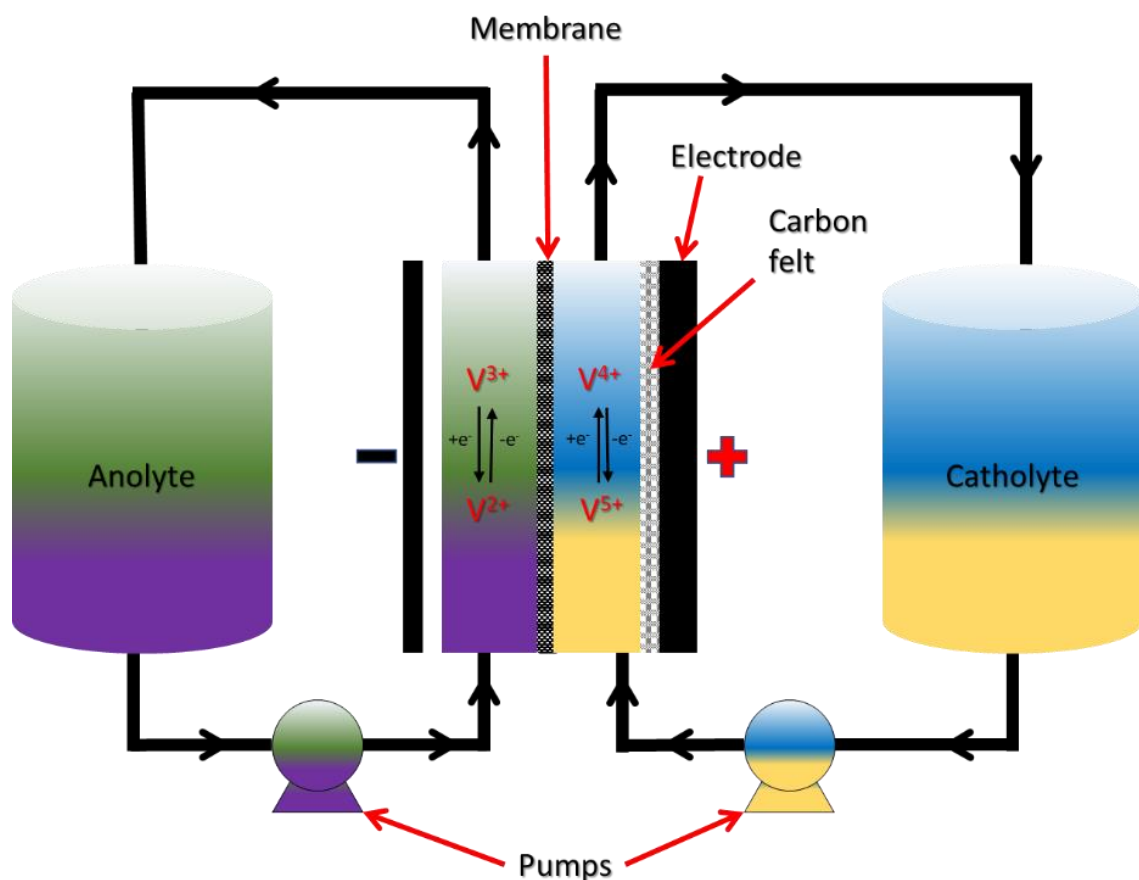
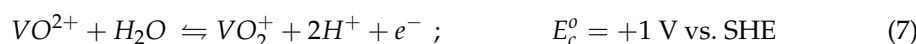


Figure 7. Schematic diagram of reactions in a vanadium redox flow battery.

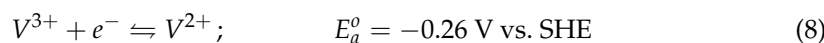
3.1.1. Chemistry of VRFB

The main reactions that occur in the battery during charge and discharge cycles are [106] as follows:

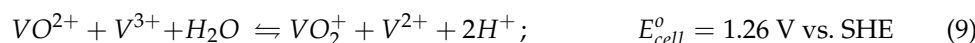
Cathode:



Anode:



Overall process:



Note [106]: $VO^{2+} = V^{4+} + O^{2-}$; $VO_2^+ = V^{5+} + 2(O^{2-})$.

The standard cell potential is 1.26 V at 25 °C, but the practical single cell voltage is between 1.4 and 1.6 V for a 1.6 M vanadium ion solution with 4.6 M sulfuric acid. VRFB net efficiency can be as high as 85%. Like other flow batteries the power and energy ratings of VRFBs are independent of each other. A typical charge–discharge curve for the VRFB bipolar electrode is shown in Figure 8 for a battery with 80% voltaic efficiency (VE) and 91% Coulombic efficiency (CE) [107]. The water (H_2O) and protons (H^+) are required in the positive reaction to maintain the charge balance and the stoichiometry [3].

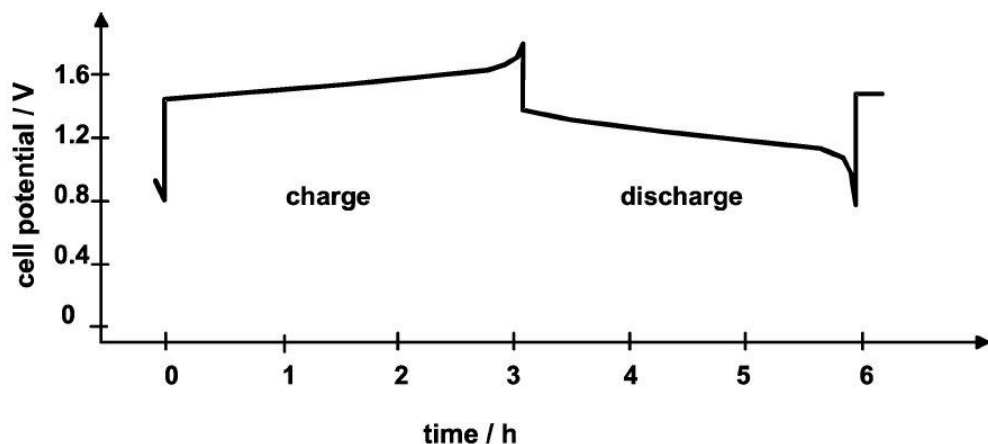


Figure 8. Typical charge discharge behaviour in a vanadium battery based on Gen 1 electrolyte (charge and discharge current = 40 mA/cm²) [107].

The discharged electrolyte contains an equal amount of V^{3+} and V^{4+} ions in single or mixed acids [108]. It is usually termed a V^{3+5+} electrolyte. During the charge cycle, V^{4+} oxidises to V^{5+} in the positive compartment, and V^{3+} reduces to V^{2+} in the negative compartment and vice versa on discharge (Table 4). H^+ ions are exchanged through the ion selective membrane [3].

Table 4. Vanadium ions with their corresponding salt, their corresponding battery state, the electrolyte state, and whether the concentration of vanadium ions increases or decreases during the charge and discharge cycle.

Species	Salt	Battery state	Electrolyte	Charge	Discharge
V^{2+}	VSO_4	Charged	Anolyte	↑	↓
V^{3+}	$V_2(SO_4)_3$	Discharged	Anolyte	↓	↑
VO^{2+} (V^{4+})	$VOSO_4$	Discharged	Catholyte	↓	↑
VO_2^+ (V^{5+})	$(VO_2)_2SO_4$	Charged	Catholyte	↑	↓

3.1.2. Different VRFB Generation Chemistries

Since the development of VRFBs in the 1980s, the VRFB electrolyte has been constantly improved and several generations of VRFBs have emerged over decades of work aimed at enhancing performance and solving challenges in operating the batteries [109]. The main differences between these generations are the use of different electrolyte chemistries or the use of a single or mixed inorganic acid [3,110] (Table 5).

Table 5. Comparison of each generation of VRFBs [101,111].

	Gen1	Gen2	Gen3
Electrolyte	V/sulphate in both half-cells	V/HBr/HCl solution in both half-cells	V/H ₂ SO ₄ /HCl in both half-cells
Negative couple	V ³⁺ /V ²⁺	V ³⁺ /V ²⁺	V ³⁺ /V ²⁺
Positive couple	V ⁵⁺ /V ⁴⁺	Br/ClBr ₂	V ⁵⁺ /V ⁴⁺
Maximum vanadium concentration	1.5–2 M	2.0–3.5 M	2.0–2.7 M
Supporting electrolyte	H ₂ SO ₄	HBr and HCl	H ₂ SO ₄ and HCl
Specific energy	15–25 Wh kg ⁻¹	25–50 Wh kg ⁻¹	25–40 Wh kg ⁻¹
Energy density	20–33 Wh L ⁻¹	35–70 Wh L ⁻¹	35–55 Wh L ⁻¹
Operating temperature range	10–40 °C	0–50 °C	0–50 °C

The second-generation VRFB (G2 VRFB) was developed to replace the V⁵⁺ /V⁴⁺ pair in the positive side with the V/HBr/HCl electrolyte, aiming to widen the operational temperature range and increase the energy density of the VRFB. Subsequently, Pacific North-Northwest Laboratories proposed using an acidic mixture (H₂SO₄ and HCl) to improve the solubility of vanadium ions in the electrolyte, leading to superior performance and higher energy density, known as the third-generation (G3 VRFB) [101]. Despite the enhanced energy density of both G2 and G3 compared to G1, the use of halides in the electrolyte increased the risk of bromine and chlorine gas evolution during operation, which increases the risk associated with the battery as well as the potential environmental impact. Currently there have been no reports of large-scale installations of G2 and G3.

3.1.3. Advantages and Disadvantages

VRFBs have discharge duration times up to 24 h. The technology has a quick response (faster than 0.001 s) with the number of maximum cycles varying in the literature, with an operational plant reporting up to 200,000 cycles over a 3 year period [112]. However, the most common number reported is 20,000 cycles [113–116]. The VRFB is the only RFB that has been used in large-scale applications around the world (Europe, Southeast Asia, and North America) for extended periods of time [55,58,117–125].

There are still technical challenges for VRFBs, including low electrolyte stability and solubility leading to low energy density [112,126]. Commercial systems are recommended to operate between 10 °C and 40 °C to avoid vanadium precipitation that can block flow channels. However, recent findings have suggested that when the SOC of the electrolyte is reduced to 70–80%, the temperature can be increased to 50 °C. Further testing is required to optimise the operating temperature, and notable research is being conducted into the use of additives to further stabilise the electrolyte at elevated temperatures [116,127–136].

As discussed previously, one of the leading causes of electrolyte instability in RFBs is active species permeation and crossover of the ion selective membrane. In VRFB, this can lead to a decrease in anolyte/catholyte which reduces the capacity of the battery as well as the self-discharge of the active species, reducing the state of charge of the system. In addition to the crossover of vanadium species, there can be a net transfer of water across the membrane, speculated to result from the transfer of hydrate vanadium ions between the two half-cells. This also contributes to the variation in electrolyte concentration and,

if left unchecked, the rapid degradation of the system [89]. As such, significant work has been conducted to improve ion exchange membranes selectivity and performance. Sun et al. modified Nafion membranes with by introducing asymmetrical layers of tungsten oxide to hinder vanadium migration and diffusion through the ion exchange membrane. In comparison with the Nafion 212 membrane, the optimal hybrid membrane prepared with 20%wt WO_3 , demonstrated higher Coulombic efficiency (93% vs. 88%), higher energy efficiency (75% vs. 65%), and higher capacity retention (62% vs. 42%) for a VRFB cell with the same current density of 60 mA/cm^2 [137]. Other work investigated the use of graphene oxide incorporated into Nafion membrane 117. Results indicated a similar increase in performance of the hybrid membrane an increase the Coulombic efficiency (96% vs. 91%) and energy efficiency (85% vs. 80%) for a VRFB system at a current density of 80 mA/cm^2 [137]. Similar findings were reported when including carbon nitride nanosheets into the Nafion matrix [138]. Alternative anion exchange membranes based on poly(phenylene oxide) with imadazolium and bis-imadazolium cations have been investigated as an alternative to the Nafion membrane for use in VRFBs. Results show that the novel membrane outperforms the Nafion membrane and achieves an impressive Coulombic efficiency of 98.5% at a current density of 140 mA/cm^2 [95]. Continuing the development of these membranes among others and evaluating the industrial application of this technology is critical to improve the longevity and widespread application of VRFBs.

In VRFBs, the carbon/graphite felt electrodes are critical in ensuring efficient electrochemical reactions. As such, significant research has been conducted to ensure that the felt electrodes have low resistance and are hydrophilic. Previous work has shown that electrochemically depositing bismuth onto the graphite felt induced better catalysis of the $\text{V}^{3+}/\text{V}^{2+}$ reaction, and the voltaic efficiency was 9.47% higher compared to pristine felt at a current density of 80 mA/cm^2 [139]. Other studies have evaluated the electrocatalytic effect of oxygen functionalisation of thermally pretreated graphite felt on the kinetics of the reactions in a VRFB. Positive effects from oxygen functionalisation as a result of thermal modification of the felt at a temperate range of 400–600 °C was observed for the negative electrode, whereas the positive electrode reaction demonstrated minimal benefits [140]. The effects of oxygen functionalisation are highly debated with contrasting results. Variation in results could be due to the amount and type of oxygen groups present [140–146]. A study by Esteves et al. demonstrated a dual oxidation approach using oxygen plasma followed by treatment with hydrogen peroxide to impart functional groups onto the graphite felt. By varying the oxidative techniques, they were able to study the effects of different oxygen groups. Results showed that O-C=O groups improved cell performance whereas the C-O and C=O groups degrade it. The increase in performance was attributed to a reduction in the cell overpotential after functionalisation. Regardless of the approach utilised, ensuring the optimal performance of graphite felt is critical in developing a functioning VRFB, and research continues to demonstrate novel applications [143,147].

Vulnerability of the storage systems to sealing and leakage issues is also a challenge [148]. The other major challenge for VRFB systems is their capital cost, roughly \$550–600 per kWh, which is high for broad market penetration [149–151]. The high cost is, in part, due to the use of relatively expensive vanadium [152,153] and the high costs of membranes, but the high initial cost can be recouped as VRFBs can operate for over 20,000 full cycles and their lifespan can exceed 20 years [3,148,150].

The International Renewable Energy Agency (IRENA) reported the advantages and disadvantages of VRFBs (Table 6) [148].

Table 6. Advantages and disadvantages of VRFB electricity storage systems [3,148,154,155].

Advantages	Disadvantages
<ul style="list-style-type: none"> • Long cycle life (20,000 + full cycles). • Relative high energy efficiency (up to 85%). • One of the most mature flow batteries with multiple deployments at MW scale. • Design E/P ratio can be optimised to suit specific application. • Long-duration (1–20 h) continuous discharge and high discharge rate possible. • Quick response times. • Same element in active materials on electrolyte tanks limits ion cross-contamination. • Electrolyte can be recovered at end of project life. • Heat extraction due to electrolyte prevents thermal runaway. 	<ul style="list-style-type: none"> • Low electrolyte stability and solubility limit energy density, and low specific energy limits use in non-stationary applications. • Precipitation of V_2O_5 at electrolyte temperatures above 40 °C can reduce battery life and reliability, although this can be managed by controlling SOC. • High cost of vanadium and current membrane designs. • Unoptimised electrolyte flow rates can increase pumping energy requirements and reduce Energy efficiency. • Poor selectivity in ion exchange membranes can lead to self-discharge and decrease in VRFB capacity. • Graphite electrodes require pre-treatment and functionalisation to perform optimally.

VRFB flow battery technology provides a very long operational life, low lifetime costs, and low greenhouse gas emissions. The battery technology is mature, and it can be considered to be at the commercial stage for fixed applications. The technology is well proven and is undergoing demonstration as a load levelling battery for electricity utility zone substations and other transmission and distribution applications [156]. VRFBs providing MWs in power and MWhs in energy storage capacity have been demonstrated, and, recently, a 200 MW/800 MWh VRFB was built and partially operated at 100 MW/400 MWh in north-east China in Dalian [157]. H₂ Inc., a South Korean VRFB company, has installed several VRFB systems and has begun construction of a factory with 330 MWh annual manufacturing capacity [158]. Sumitomo, in Hokkaido, have a plant operating at 17 MW/51 MWH [157].

3.2. Iron Chromium RFBs

The iron-chromium redox system was initially investigated by NASA [40] and is the basis of one of the earliest proposed RFBs (Sun and Zhang, 2022). The hydrochloric acid-acidified aqueous solutions contain a ferric-ferrous redox couple and a chromium-chromic couple that serve as the positive and negative reactants, respectively [159]. Each reactant in this redox flow cell flows at a rate that is consistently higher than the stoichiometric flow requirement, allowing all the reactants to be used up in one cycle through the cell. The two flowing reactant solutions are divided by an anionic and cationic ion exchange membrane in each cell [159].

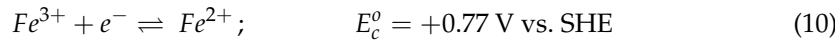
In theory, the membrane prevents the cross-diffusion of the iron and chromium ions, allowing only the chloride and hydrogen ions to freely move through the cell to complete the electrical circuit [159]. The performance of a Fe-Cr redox flow cell was investigated by a number of researchers and organisations, including NASA [40,160–162], a study team at the University of Alicante in Spain [160], and Shimada et al. [163], who reported that the Coulombic efficiency of a redox flow cell increased to 95% when the carbon structure in the electrodes was changed from amorphous to graphite. As with VRFBs, the electrode treatment is critical to ensure efficient battery operation.

In a recent study by Wu et al. [164], the significant capacity loss observed in iron-chromium redox flow batteries (ICRFBs) was analysed, highlighting its hindrance to further technological advancement. The authors attributed this loss to the presence of inactive $Cr(H_2O)_6^{3+}$ ions, leading to an imbalance in active ion content between the catholyte and the anolyte. To address this issue, a novel electrolyte formulation was introduced, increasing the Cr concentration from 1 M to 1.3 M. This modification resulted in an energy efficiency (EE) of 84.51%.

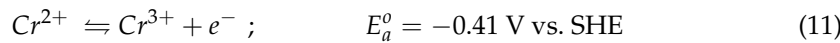
3.2.1. Chemistry of Iron Chromium RFBs

The electrolyte used in ICRFBs contains chromium on the anode side and iron on the cathode side. The separate redox reactions are listed below. The ICRFB produces a standard voltage of 1.18 V [159,165,166].

Catholyte:



Anolyte:



Due the fast kinetics of the Fe(II)/Fe(III) redox reaction, only carbon felt is typically required. However, the Cr(II)/Cr(III) redox reaction is slower, and, for an efficient design, a catalyst is required to enhance the electrochemical kinetics. It is essential for the catalyst to have a high overpotential towards hydrogen evolution as, thermodynamically, hydrogen is more easily reduced than the Cr(III) species [159,165]. If this occurs, the cell will have a reduced Coulombic efficiency as well as an imbalance of the state of charge between the catholyte and anolyte solutions, resulting in a rapid capacity decay [159]. Typical catalysts include Bi and Au-Ti, which are deposited on the electrode surface to enhance the electrochemical kinetics of the chromium redox couple [60]. In addition to the use of catalysts, a rebalance cell can be utilised to rebalance the SOC of the electrolyte [60].

3.2.2. Advantages and Disadvantages

In addition to the general advantages and disadvantages associated with RFBs, the iron-chromium ICRFB presents a distinct set of benefits and challenges specific to its operational context. A primary advantage of ICRFB technology is that its active species— Fe^{2+}/Fe^{3+} and Cr^{2+}/Cr^{3+} —are non-toxic to both humans and the environment [159]. Operating within a temperature range of 40–60 °C, ICRFB systems are particularly well suited for warmer climates, such as those found in many regions of Australia [159]. Furthermore, ICRFB exhibits relatively low resistance, comparable to that of conventional Generation 1 VRFBs, due to the high conductivity of hydrochloric acid, which serves as the supporting electrolyte. The use of mixed active species, in contrast to single-active-species systems like VRFBs, offers additional advantages. Notably, a highly selective permeable membrane is not necessary, which significantly lowers capital costs [159,167]. Additionally, the chemical production costs associated with chromite ore may be lower than those for pure chemicals, as the separation of iron and chromium is not required. However, accurate cost estimates per kWh are currently unavailable due to the absence of large-scale applications of this technology [159].

Since graphite felt has an important role in ICRFBs and VRFBs, significant research has been dedicated to improving the catalytic effect of the electrodes. One of the earlier examples of this is an investigation by Johnson and Reid [168] where the Fe-Cr redox system was assessed using electrodes made of 1/8 inch carbon felt, and the felt in the chromium half-cell was modified by the inclusion of 12.5 µg/cm² of gold. More recently, Niu et al. utilised silicic acid etching to intricately carve dense nano-porous structures onto the surface of carbon cloth electrodes. This innovative technique resulted in a remarkable achievement, with the battery attaining an average energy efficiency of 81.3% [169]. Chen et al. demonstrated the inclusion of SiO₂-decorated graphite after silicic acid etching which resulted in significant improvement in battery performance. The SiO₂ introduced by the decomposition of silicic acid can increase the effective specific surface area of the graphite felt while also facilitating the oxidation of the felts at 500 °C. A significant increase in the oxygen functional groups was observed and treatment the negative reaction

activity of the ICRFB and voltaic efficiency increased by 6.61% at a current density of 120 mA/cm^2 [170]. Similar results have been observed with boric acid etching of graphite felt followed by thermal treatment at 500°C , after which the energy efficiency of the ICRFB cell was increased by 9.5% compared to pristine felt [171]. Zhang et al. extensively studied the impact of the oxygen functional groups, the impact of graphitisation degree, and the surface area of both carbon felt and graphite felt. Both electrodes were investigated with and without BiCl_3 as a catalyst. It was found that graphite felt outperformed the thermally treated carbon felt due to the higher degree of graphitisation. In addition, although bismuth ions are believed to have the dual effect of inhibiting the hydrogen evolution reactions and catalysing the negative electrode reactions, the shorter catalytic path by oxygen functional groups is of greater benefit to improve the stability of ICRFBs [172]. There is an extensive range of treatment options to ensure excellent performance of the graphite felt in general. These can be broadly categorised as either modification of surface functional groups or modification of surface catalytic materials. Both options have been shown to be effective, and the application of the specific method would depend on the battery chemistry involved [173]. The necessary treatment of the graphite felt in an ICRFB can be a disadvantage, but as discussed, significant research has been performed to address this issue.

Despite these advantages, several disadvantages accompany the implementation of ICRFBs. The permeation of all active species through the membrane can create substantial concentration gradients between the anode and cathode tanks, resulting in decreased performance and accelerated degradation of the electrolyte [159]. The mixed electrolyte also exhibits reduced solubility, which limits the overall capacity of the system. While the solubility of FeCl_2 and CrCl_3 can reach 2 M, the solubility in the mixed system is considerably lower, with optimal electrolyte concentrations reported at 1 M FeCl_2 , 1 M CrCl_3 , and 3 M HCl [174]. Additionally, the system operates within a narrow voltage range of 0.7–1.2 V, further constraining its capacity [174]. The standard potential of the $\text{Cr}^{2+}/\text{Cr}^{3+}$ couple is close to that of hydrogen evolution, which can trigger parasitic side reactions, diminishing capacity and exacerbating electrolyte imbalance [159]. Although some of these issues may be mitigated through rebalancing systems, such solutions increase both the cost and complexity of maintenance for the system. Figure 9 provides an overview of an ICRFB cell [166].

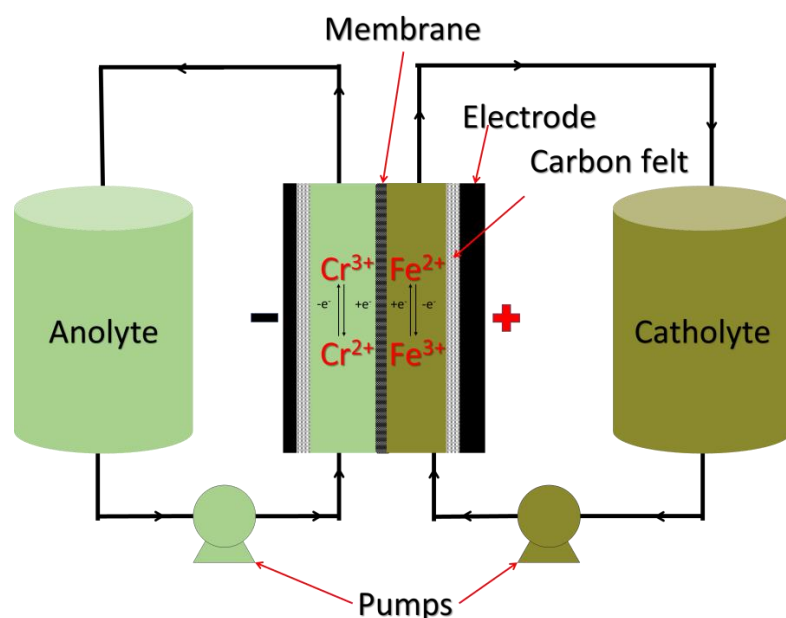


Figure 9. Schematic diagram of operation of an iron chromium redox flow battery cell.

3.3. Polysulphide RFBs

A polysulphide bromide battery (PSRFB) is a type of RFB that uses sodium bromide and sodium polysulphide as salt solution electrolytes. Extensive research efforts have been dedicated to PSRFB systems over numerous years [175]. Polysulphide redox species demonstrate excellent solubility in aqueous solvents, leading to their wide use in RFBs containing sulphur [176,177]. The solution chemistry of PSRFBs is governed by the intrinsic properties of the polysulphide compounds and their interactions with solvent molecules, which dictates the system design and cell architecture [176]. The reversibility of the formation of different polysulphide species is susceptible to the influence of different cations such as Na^+ , Li^+ , and K^+ , and this needs to be taken into consideration in cell design [176]. PSRFBs can be classified as all liquid or hybrid systems, where hybrid systems include liquid/solid, semi-solid, and liquid/gas systems. The chemistry of PSRFBs is complex and depends not only on the polysulphides but also on the solvents used and the type of system.

3.3.1. Chemistry of Polysulphide RFBs

The chemistry of PSRFBs is governed by the polysulphides which undergo reversible anodic and cathodic reactions. As with other RFBs, the electrolyte is pumped from separate anolyte and catholyte tanks into a cell where the half reactions take place [178]. The exact reactions that take place are dependent on the polysulphide species and solvent present, but an example of a sodium polysulphide RFB is shown in reactions 12–14 [176]. During the discharge, short chain polysulphides and the sulphide solution are pumped into the anodic half-cell to be oxidised to high chain polysulphides. In the cathodic half-cell, bromine is reduced to bromide with the charge compensation by the Na^+ ion. An overview of a sodium bromine polysulphide batteries can be seen in Figure 10, and the reactions involved are the following [176]:

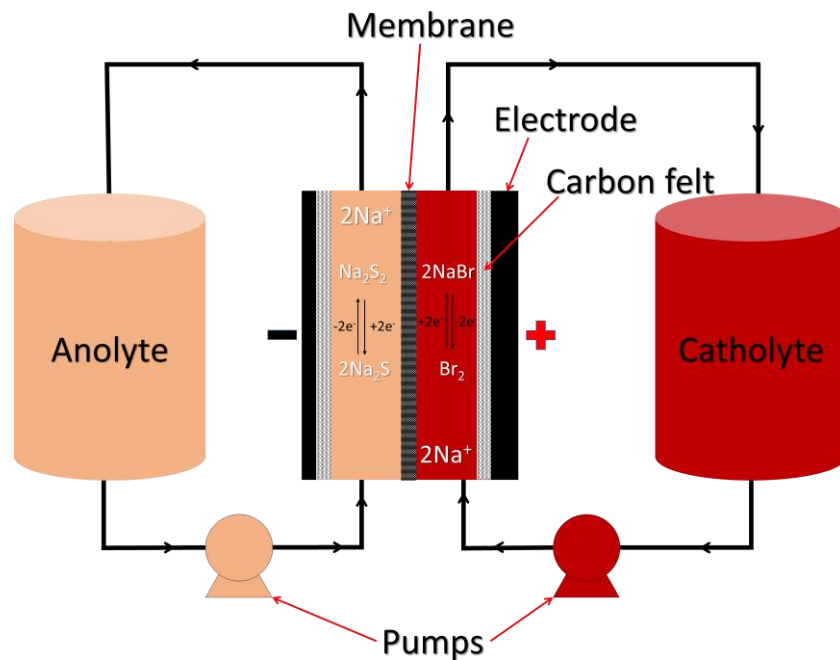
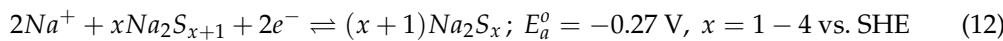


Figure 10. Schematic diagram of operation of a sodium-bromine polysulphide redox flow battery where $x = 1$ (Reaction 14).

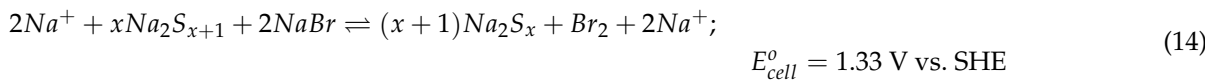
Anode:



Cathode:



Overall:



All Liquid PSRBs

In all liquid PSRBs, the electroactive species are dissolved in solvents to form the electrolyte. There are a range of solvents that are suitable for use. The commonly used solvents include 1,2-dimethoxyethane (DME)/1,3-dioxolane (DOL) [179], dimethylsulfoxide (DMSO) [180], and tetrahydrofuran (THF). The choice of solvent is important as the interaction between the solvent and the polysulphide will dictate the potential window where the cell operates. For example, water can be used as an inexpensive solvent for PSRBs; however, it has a limited electrochemical window [176]. During cell operation, hydrogen- and oxygen-evolving reactions occur, leading to the rapid decay of the electrolyte. In addition, water and sulphur can also generate unwanted species such as hydrosulphide and hydrogen sulphide under certain pH conditions. The use of organic solvents results in a larger potential window but has the drawback of increased cost [176].

In the aqueous system, the chemistry of the cell is dependent on the electrochemistry of the solvent and polysulphide species, the temperature, and the interaction between polysulphides and the solvent. Short chain polysulphides (S_n $1 \leq n < 4$) are preferred as they favour high conductivity; however, these cells often have low theoretical capacity [181]. In addition, these ionic systems have intermediate sulphur species (S_n^{2-}) that convert to HS^- and OH^- through hydrolysis of the electrolyte [176]. As such, careful control of the redox potential of the electrolyte is essential to help prevent the formation of these species and hydrogen and oxygen evolution reactions. Various studies have investigated mechanisms to increase the electrochemical stability window of these electrolyte solutions.

Hybrid PSRBs

Hybrid PSRF systems can be further divided into solid/liquid, semi-solid, and liquid/gas systems. These systems have been designed with the intention of increasing the theoretical capacity of the batteries and creating a more electrochemically stable system in comparison to aqueous PSRBs.

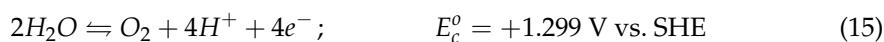
Solid/liquid PSRBs take advantage of the high energy density of lithium metal to create high-capacity systems that are easily scalable. In these systems, long chain polysulphides are often dissolved in organic solvents to form the catholyte in conjunction with metals such as lithium [180]. However, intermediate sulphur species can react with the lithium species to form short chain lithium sulphides that precipitate out of the solution, resulting in loss of active material and overall decay of the system [182].

Semi-solid PSRBs have been proposed as another alternative to aqueous systems. These systems utilise redox-active material suspensions instead of solutions, which have the advantage of increasing the concentration of redox active species past the point of solubility, thereby creating a more energy dense system [176]. Metals commonly used include $LiFePO_4$, $LiNi_{0.5}Mn_{1.5}O_4$, and $LiCoO_2$ suspended in an electrolyte solution [183]. In addition, nanomaterials can be introduced into the system to improve the reaction rate of the polysulphide redox species [184]. These systems offer the benefits of higher efficiency, capacity, and cycle life compared to aqueous systems. However, the active materials are more expensive than those used in aqueous systems [176].

Liquid/Gas PSRBs

A key strategic advantage of RFBs is the ease of scalability and low cost of the system. Although semi-solid PSRBs have addressed many issues associated with the use of polysulphides, the overall cost of the system is significantly higher due to the use of expensive metals in the catholyte [176]. Liquid/gas PSRBs have been proposed as an alternative solution that removes the need for expensive metals in the catholyte. These RFBs pair a polysulphide anolyte with an oxygenated salt solution as the catholyte. At the anode side, the reaction proceeds as described in reaction 16 and 18. However, at the cathode side, an oxygen layer is introduced that promotes oxygen evolution/reduction in the redox active species in the catholyte [185]. In this configuration, two half reactions are paired, specifically, polysulphide oxidation and the oxygen evolution reaction (OER) and oxygen reduction reaction (ORR). The half reactions taking place vary depending on the pH of the catholyte, as described in reactions 15 to 18 [185].

Acidic catholyte:



Acidic anolyte:



Basic catholyte:



Basic anolyte:



To maintain electroneutrality, metal ions such as Na^+ and Li^+ are consumed or generated through oxygen electrochemistry. As such, the efficiency of the cell is dependent on the total concentration of metal ions in the catholyte and the concentration of polysulphides in the anolyte [185].

This design has a lower cost compared to that of the other hybrid PSRBs; however, there are still many challenges for this design that require additional research. Specifically, the generation and consumption of H^+ (for an acid catholyte) or hydroxyls (for an alkaline catholyte) lead to pH swings in the catholyte. In addition, the ORR and OER reactions are inefficient, reducing the economic viability of the design [176].

3.3.2. Advantages and Disadvantages

PSRFB typically have high solubility (up to 8.8 M) and low cost; however, the many versions of PSRFB have been developed in an attempt to address some of the key disadvantages of the technology [186]. When the technology was first proposed in 1983, aqueous solutions of sodium bromide and sodium polysulphide were used. Compared with some other RFB, the polysulphide bromide batteries were less expensive; however, the system had a decrease in power density and energy efficiency [186]. This is because the cation exchange membranes in the Na^+ form have higher ohmic resistance compared to the H^+ form [187]. This limited the use of high current densities. In addition, the S_{n-1}^{2-}/S_n^{2-} redox reaction is characterised by retarded electron transfer, requiring the use of cobalt or a nickel-based catalyst on the electrode to facilitate efficient electron transfer, increasing the cost of the system. The initial system also had potentially significant environmental impact due to the presence of bromine compounds [187].

Over the course of its development, many of these issues in PSRFB were addressed by substituting bromide compounds for other halides. The cost of the system can also be reduced by using less expensive redox couples with minimal environmental impact, such as the use of I_3^-/I^- with the S_{n-1}^{2-}/S_n^{2-} couple [188]. The theoretical energy of such a system with 6 M KI and 3.3 M K_2S_2 solutions is 85.4 W h L⁻¹; however, the reported capacity was much lower at 49.4 W h L⁻¹ [188]. The system reported an energy efficiency of 63–73%, a voltaic efficiency of 73–78%, and a Coulombic efficiency of 86–93%. However, the performance of this system is still poor compared to other RFBs, and the issues with the high ohmic resistance of the membrane and the costs associated with the use of catalyst is still an issue.

3.4. Organic RFBs

Recently a new type of RFB, organic redox flow batteries (ORFB), have gained an increasing amount of interest [189,190]. ORFBs utilise redox-active organic molecules and polymers instead of inorganic molecules used in other RFBs. Methods such as molecular engineering allow a range of different organic compounds to be constructed, each with unique physical, chemical, and electrochemical properties [189]. As a result, ORFBs have a large amount of diversity stemming from the range of different organic molecules that can be utilised.

The first redox-active organic electrolyte was tested in 2009 when tiron (4,5-dihydroxy-1,3-benzenedisulfonic acid) was coupled with lead to form a Pb/tiron aqueous hybrid flow battery [191]. Since then, many more redox-active species have been investigated [189,190,192,193]. Competitive organic electrolytes typically feature highly negative or positive redox potential, high water solubility, high structural stability, rapid redox reaction kinetics, and low cost [190]. The redox-active species can be tailored through either change in the structure of the molecules themselves or through the addition of additives. For example, to acquire high potential differences, electron withdrawing groups such as $-NO_2$, $-SO_3^-$, and $-PO_3^{2-}$ can be added to catholyte compounds. Electron donating groups such as $-NH_2$ and $-OH$ can be grafted with anolyte compounds [190]. By adding additives, the solubility of redox active species can also be increased. For example, flavin mononucleotide in 1 M KOH can be increased from 0.1 to 1.5 M by the addition of 3 M vitamin B3 [194].

A key advantage of ORFB is that potential redox couples can be designed with the help of computational modelling and the behaviour of these compounds predicted [189,190]. These compounds can feature high energy density (210 W h dm⁻³) [189] and high charge capacity (320 A h dm⁻³) [189] with some species reporting low crossover [190]. As such, ORFBs hold great promise for industrial application. However, there are still many challenges that need to be addressed. While many organic molecules show high solubility in water, they show very poor solubility in supporting electrolytes (made from inorganic salts) due to the salting out effect [190]. In addition, most of the reported electrolytes have had limited amounts of attention, and parameters such as pH [195,196], viscosity [194], temperature [197], and the range of SOC [198] still require optimisation. The physical construction of the cell, and, in particular, the membrane, still need to be further investigated and optimised [199]. In addition, although aqueous redox flow batteries generally can be considered non-flammable, the application of the electroactive organic species in ORFBs is still comparatively new, and the associated hazards will need to be investigated on a case-by-case basis. However, further research ORFBs can be adapted for industrial use. Despite a significant amount of research in the area recently, there is a notable lack of mature ORFBs, complicating the assessment of long-term advantages and disadvantages of the technology. Currently, there is no Australian industrial application of the ORFB.

4. Hybrid RFBs

4.1. Zinc Bromine RFBs

The zinc bromine battery (ZBB) is termed a hybrid flow battery because one of its electrodes, zinc, participates in the reaction after charging. Currently, this technology is being developed primarily for stationary energy storage applications [3]. The system has an excellent energy capacity (specific energy density is 65–84 Wh/kg).

The ZBB concept originated in the 1880s [200], but due to technical difficulties, particularly with bromine corrosiveness, its development was not fully realised until the mid-1970s. ZBBs have attracted the interest of researchers as a rechargeable power source due to their high energy density, high cell voltage, high degree of reversibility, and use of readily available, low-cost materials. The electrolyte is a zinc bromide salt dissolved in water, and, during charging, zinc is plated on the negative electrode, which limits the capacity of the battery [3].

Capturing the bromine produced at the positive electrode during charging is imperative due to its high solubility in the aqueous electrolyte, which poses constraints on turnaround efficiency and longevity. Various methodologies have been proposed to mitigate bromine concentration in the electrolyte and alleviate self-discharge, including complexation of generated bromine with chemicals or dissolution in organic solvents. Singh et al. [84,201] suggested the utilisation of an organic solvent where a bromine/propionitrile solution forms a biphasic system with high conductivity and favourable charge–discharge characteristics. Bloch et al. [202] investigated the reaction between low molecular weight tetraalkylammonium halides and bromine-containing aqueous solutions to produce sparingly soluble polyhalides. The complexation of bromine, generated during the charging process, with quaternary ammonium salts allows for the binding of up to nine bromine atoms per molecule [203], thereby significantly lowering the bromine vapour pressure [85] to levels similar to that of brominated zinc bromide solutions [203]. This results in an exceptionally low concentration of free bromine in the electrolyte, as the majority of the bromine exists either as polybromide ions dissolved in the aqueous phase or bound to complexing agents in a secondary phase. Under these complexed conditions, both the chemical reactivity and the evaporation rate of bromine are markedly reduced relative to its elemental state. In a recent study, ref. [204] introduced a new additive of soft-hard zwitterionic trapper that complexed bromine to form a polyhalide-complexing ‘soft’ cationic and a water-soluble ‘hard’ anionic. The generated polybromide reduces the bromine crossover and generates a homogeneous aqueous solution free from phase separation. Presently, zinc bromine flow batteries (ZBFBs) employ quaternary ammonium salts such as N-Ethyl N-methyl pyrrolidinium bromide and/or N-ethyl-N-methyl-morpholinium bromide to complex bromine [50,205]. Recently, a Prussian blue-modified nitrogen-doped carbon (PB@NC) has been engineered as a redox-targeting catalyst for the bromine cathode, facilitating improved electron transfer and increasing bromine species concentration at the reaction interface. This modification enables Prussian blue to rapidly undergo redox transformations, thereby enhancing the electrochemical kinetics and overall efficiency. Consequently, ZBFBs employing PB@NC demonstrate an energy efficiency of 85.9% at a current density of 80 mA cm^{-2} and 71.1% at 160 mA cm^{-2} . This work highlights a promising strategy for optimising the performance of ZBFBs through the innovative design of cathode materials [80].

At the negative electrode, zinc is redissolved to form zinc ions, and bromide ions are formed during discharge at the positive electrode [3]. To recirculate the bromine complex, a third pump or extra valve is required. The efficiencies of ZBFBs range from 60 to 75%. In terms of energy output, ZBFBs ranging from 500 kWh to 2 MWh have been built and tested over the years [46–49,51,81].

4.1.1. Chemistry of Zinc Bromine RFBs

The chemistry of the charge and discharge of ZBBs can be summarised using reactions 19–22 [82,83]. An illustration of a ZBRFB cell can be seen in Figure 11.

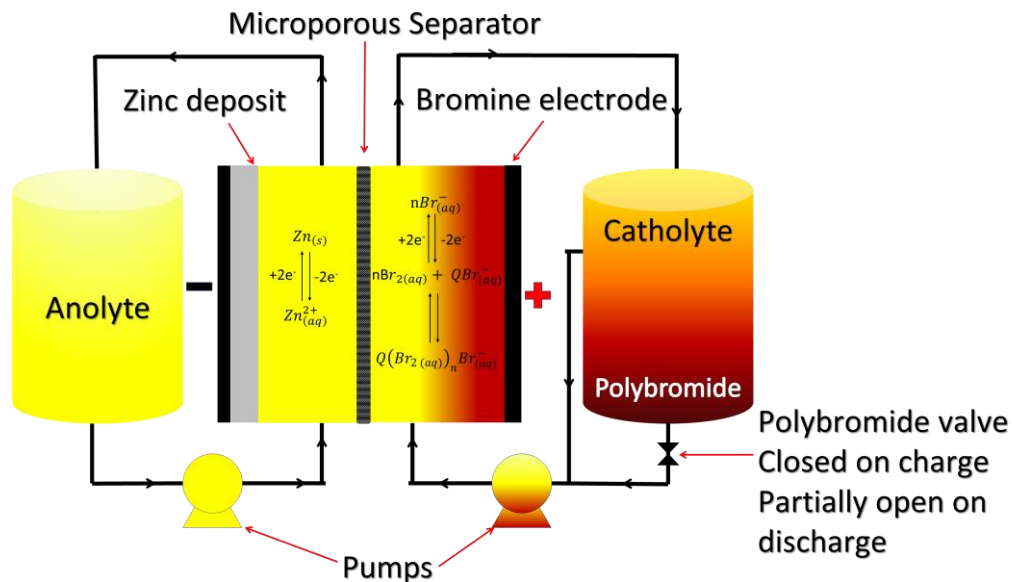
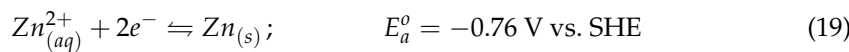
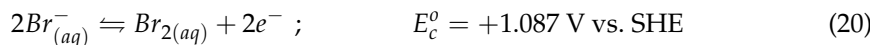


Figure 11. Schematic diagram of operation of a zinc bromine redox flow battery.

Anode:



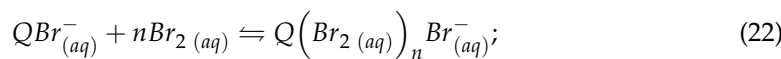
Cathode:



Overall:



Bromine Complex:



QBr^- = Complexing Agent

$Q(Br_2)_n Br^-$ = Polybromide

4.1.2. Advantages and Disadvantages

In the past, ZBFB was popular because of the low cost, readily available reagents, and excellent energy capacity. It is the second most employed RFB after VRFB.

However, there are still several key issues with the technology. During the operation of the battery, the heterogenous redox reaction of zinc can result in an uneven plating of the metallic zinc [186]. This is affected by a range of parameters such as temperature, current densities, and concentration of active material on the electrode. This uneven plating results in the formation of zinc dendrites, which can impair membrane functionality and lead to battery failure [206]. Dendrite formation is more prevalent at higher current densities and this, coupled with the slower kinetics of the active species, reduces the current densities of the battery, especially during the charging phase [186].

The plating of zinc also limits the capacity of the cell since the surface area for the electrodeposition of zinc is limited. As a result, the capacity of the battery is determined by size of the battery stack instead of the volume of the electrolyte stored in external reservoirs. Increasing the size of the zinc deposits can also increase the transport resistance. The plating of the zinc also results in a change in the ionic strength between the anolyte and catholyte [186]. As a result, water can more easily migrate across the membrane, resulting in a change in the electrolyte concentration and a level imbalance between the anolyte and catholyte [207]. Stable Zn plating and stripping are the main keys to achieve a high-capacity ZBFBs. Further research in the ZBFB, especially in developing specialised membranes, electrodes with high affinity towards zinc and bromine, and additives to prevent water migration [207], can help create a more stabilised battery [186].

4.1.3. Alternatives to ZBFB

An alternative to ZBFB, an alkaline zinc iron flow battery (ZIFB), was also investigated. The electrolyte consists of $\text{Fe}(\text{CN})_6^{4-}/\text{Fe}(\text{CN})_6^{3-}$ and $\text{Zn}(\text{OH})_4^{2-}$ active species. In 2014, ViZn Energy developed a ZIFB module with a capacity of 80 kW–160 kWh installed at Flathead Electric Cooperative [186]. In 2018, researchers demonstrated a steady ZIFB for more than 500 cycles when utilising a porous PBI membrane [208]. In 2020, the same group installed a 10 kW ZIFB system. However, the strong alkaline conditions result in not only a reduced solubility for the $\text{Fe}(\text{CN})_6^{4-}/\text{Fe}(\text{CN})_6^{3-}$ but also lead to decomposition of ferricyanide and self-oxidation catalysed by carbon electrodes [209]. By using a chelating agent, the $\text{Fe}(\text{CN})_6^{4-}/\text{Fe}(\text{CN})_6^{3-}$ species solubility could be increased to 1.7 M (from 0.4 M) in near neutral electrolytes. This resulted in a cell with an energy density of 74 Wh L⁻¹ at 60 °C [210]. This is only one of the many zinc-based flow batteries investigated in recent years. Others include Zn–I₂ [211], Zn–Mn [212,213], Zn–poly(TEMPO) [214], and Zn–Ce [215] flow batteries.

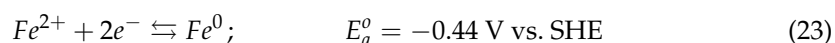
4.2. All-Iron RFBs

Hruska and Savinell [216] proposed all-iron RFBs (AIRFBs) in 1981. Similarly to all vanadium RFBs, AIRFBs benefit from using the same electroactive species in both the anode and cathode side of the cell. This eliminates concerns with cross contamination, which can degrade the electrolyte as discussed previously, as well as simplifying the electrochemistry of the cell, making it easier to control the redox active window. Since iron is one of the most inexpensive and common metals, AIRFBs are very inexpensive, with costs as low as \$2/kWh. AIRFBs can be further divided into aqueous systems or hybrid systems, each with its own advantages and disadvantages.

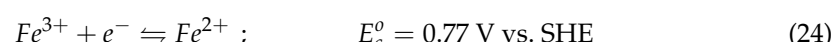
4.2.1. Chemistry of All-Iron RFBs

AIRFBs employ iron in different valence states for both the positive and negative electrodes [217]. During cell operation, the electrolyte undergoes both reduction and oxidation, according to reactions 23 and 24 [218].

Anode:



Cathode:



The three different valance states of iron make operation of AIRFBs possible. These systems are non-hazardous and inexpensive, with relatively simple engineering, which makes them good candidates for many applications [218]. A basic illustration of AIRFB operation can be seen in Figure 12.

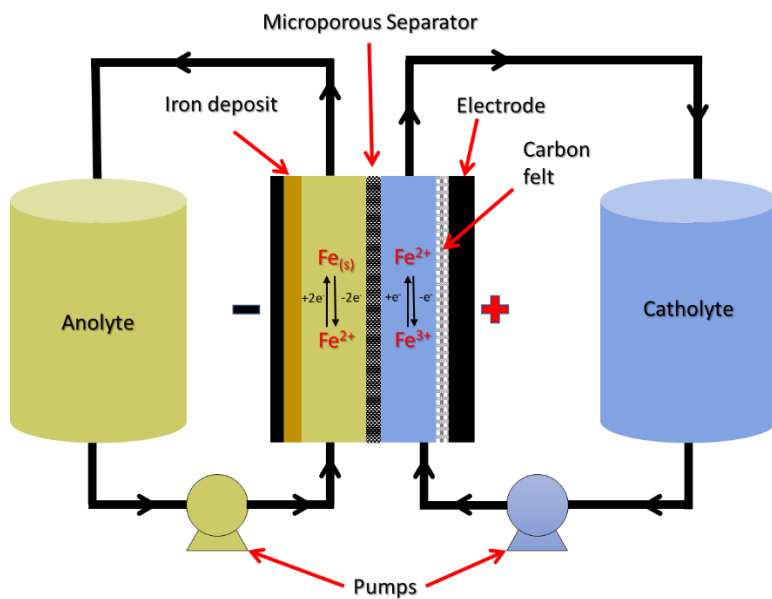


Figure 12. Schematic diagram of operation of an all-iron redox flow battery.

Hybrid AIRFBs

Hybrid AIRFBs were the first type of AIRFBs to be developed and utilise solid Fe on the anode side suspended in an electrolyte and iron in an all-aqueous electrolyte on the cathode side. The anode side is typically in the form of a slurry which increases energy density and reduces the amount of water required [219,220]. However, this comes at the expense of higher ohmic resistance due to the higher viscosity of the slurry [219,220]. As a result, the depths of the charge and discharge cycles are reduced. The Coulombic efficiency can also decrease due to crossover of the active ions through the separating membrane. In addition, Fe^0 crystals can deposit on the negative electrode to form dendrite crystals that may puncture and damage the separating membrane [219]. Overall, these effects can reduce the battery's cycling ability over time, until it ceases to operate.

Aqueous AIRFBs

To address issues with AIRFBs, including hydrogen evolution and dendrite formation, aqueous AIRFBs have been investigated. Aqueous AIRFBs utilise organic ligands to form complexes with iron ions. This allows for the use of electrochemically stable redox agents across a much larger range of conditions. For example, it has been demonstrated that an AIRFB can operate in a pH range from near neutral to pH 8.6 using iron Fe^{3+} complexed with iron(III)-N,N'-ethylene-bis-(o-hydroxyphenylglycine) on the anode side and sodium ferrocyanide on the cathode side. This system would also be environmentally friendly. Other ligands have been examined for use in AIRFBs, including organic diacids, malic acid, malonic acid, amino acids, and dimethylsulfoxide, and were found to increase iron solubility over an even wider pH range [221]. Glycine was found to be the best candidate for use in an all-iron RFB, with faster kinetics and the ability to stabilise 0.5 M iron at pH 2 [221,222]. An electrolyte with a 1:1 glycine-to-iron ratio showed a reasonable open-circuit potential of 468 mV vs. Ag/AgCl . The cell performed best when the anolyte pH was 1 and the catholyte pH was in the range 3–4. At a discharge power density of 50 mW/cm², the cell had a Coulombic efficiency of 90; although, it had a low energy efficiency (50%). It was discovered that proton reduction during cycling caused an electrolyte imbalance, but at higher cell voltages, hydrogen evolution causes the pH to rise and Fe(OH)_2 to precipitate. Currently, energy storage systems (ESS) and electric fuel are key players in the manufacturing of iron hybrid redox batteries [219].

4.2.2. Advantages and Disadvantages

Compared to other battery RFB chemistries, the all-iron batteries have some of the lowest reagent costs and have the advantage of low chemical toxicity [186]. There have been several large-scale applications of the technology. United States-based ESS Inc. (ESS) specialises in the industrial application of AIRFB. They have numerous installations, including a 10 kW/60 kWh capacity system at the California Stone Edge Farm Winery from 2016 and two 400 kWh systems for a microgrid from 2017 [186]. In addition to the low cost, AIRFBs are also easily recyclable and are environmentally friendly compared to VRFB [223].

However, there are numerous challenges that still need to be addressed. Similarly to Fe–Cr FB, the all-iron type also needs auxiliary components to ensure the system runs stably as the severe side reaction and poor $\text{Fe}^0/\text{Fe}^{2+}$ activity result in penalties in both system cost and energy efficiencies. Research has been focused on decreasing the hydrogen generation through the addition of additives such as ammonium chloride, sodium citrate, and other organic compounds [218].

The problem with organic compounds is the long-term decomposition of organic complexes over time, leading to capacity degradation and cycling instability. An alternative is to use an iron complex. Recent research demonstrated the use of such Tris(4,4'-bis(hydroxymethyl)-2,2'-bipyridine) iron dichloride in the positive electrolyte and bis(3-trimethylammonio) propyl viologen tetrachloride in the negative electrolyte. The resulting electrolyte was near neutral and demonstrated excellent cycling with a decay of only 0.07% per day over 35 days [224].

The use of sodium citrate resulted in a stable Fe^{2+} -citrate complex that increased cycling stability and achieved a near-100% Coulombic efficiency [225]. Although these additives, among others, show promise, the long-term stability has yet to be examined. More research is required to investigate the use of additives to mitigate hydrogen generation as well as stabilise the iron complex in an attempt to broaden the pH range in which the electrolyte is stable [186].

5. Suitability for Sustainable Powering of Australia

Australia, a country with vast renewable energy potential, continues to expand its solar and wind energy capacity. Correspondingly, the need for effective energy storage solutions will become increasingly critical. This increasingly turned Australia to advanced energy storage technologies to enhance grid stability and facilitate the transition to a low-carbon economy. A number of different energy storage technologies are employed across Australia, each with their own advantages and disadvantages. A summary of the different energy storage technologies is presented below.

5.1. Pumped Hydro Energy Storage

PHES, pumped hydro energy storage, is a method of storing energy by using two reservoirs of water at different elevations. During periods of low electricity demand, excess energy is used to pump water from the lower reservoir to the upper reservoir, effectively storing potential energy. When electricity demand is high, the stored water is released back into the lower reservoir through turbines, generating electricity. This process can be repeated, making it a reliable and efficient way to balance supply and demand in the power grid [226].

PHES is the world's largest energy storage technology, contributing 96% of the total global energy storage capacity [226]. Approximately 616,000 potential sites for PHES have been identified with over 23,000 TWh of potential energy storage capacity [227]. Over 160 countries have some form of PHES. It has significant advantage over other energy storage technologies in scale, with typical operation ranging from 10 to 4000 MW, and

robustness and longevity (40–60 years) [226]. However, due to the significant amount of infrastructure requirements, the cost of PHES is comparatively high at 2000–4300 \$ kW. Due to the complexity of PHES, the lead time is typically 5–12 years depending on the location [226,227].

In Australia, PHES provides 5–7% of total electricity [228]. There are over 120 operating hydroelectric power stations, concentrated mostly in southeastern Australia [228]. There are three PHES projects connected to the national electricity grid: Wivenhoe Dam, Tumut 3, and the Shoalhaven power stations, together amounting to 1.6 GW. One of the newest projects under construction is the Borumba Hydro Project in Queensland, Australia. The project is expected to provide 2000 MW of storage with the project commencing in 2022. However, the lead time is 7 to 10 years and is expected to cost \$12–14 billion AUD [228].

Although some studies have determined that Australia has adequate PHES sites to support a 100% renewable energy market, the future of the market remains uncertain. The economic viability in a rapidly changing market is a large hurdle and the long-term impact of climate change on water sources is a concern. Although suitable for medium- to long-term storage, the technology is not suitable for smaller scales and remote locations such as mining sites [226].

5.2. Solid Gravity Energy Storage Systems

Gravity energy storage systems, also known as gravitational potential energy storage, operate by using surplus energy to lift a mass, typically water or solid weights, to a higher elevation. This stored potential energy can be converted back into electrical energy when the mass is allowed to descend, driving a generator in the process. These systems are highly efficient, environmentally friendly, and provide a reliable way to balance energy supply and demand. However, their implementation requires significant infrastructure and suitable geographical locations, which can limit their widespread adoption [229]. There are currently no full-scale applications of solid gravity energy storage systems in Australia; however, Green Gravity has recently raised \$9 million dollars in funding from investors to explore the application of this technology at an old mine site, Yancoal, in New South Wales [230]. The company states that they expect the technology to be suitable for mid duration storage applications of 4–24 h and deliver an energy efficiency of up to 80%.

5.3. Fly Wheel Energy Storage

Flywheel energy storage (FES) systems work by converting electrical energy into kinetic energy through a rapidly spinning rotor or flywheel. When energy is needed, the rotor's kinetic energy is converted back into electrical energy by a generator. The flywheel is housed in a low-friction environment to minimise energy loss, allowing it to maintain its rotational speed efficiently. This method provides quick energy release and is ideal for short-duration energy storage and stabilisation of power grids.

It is characterised by high power density, quick response times, and high energy efficiency; however, it has comparatively high capital costs and the moving parts are susceptible to failure under the high operational speeds associated frequent use. In Australia, there has been very limited adoption of FES (32 kWh) [231].

5.4. Green Hydrogen Energy Storage

Green hydrogen energy storage involves producing hydrogen through electrolysis, which uses renewable energy sources like solar or wind to split water into hydrogen and oxygen. The hydrogen is then stored in pressurised tanks or underground caverns until needed. When energy demand rises, the stored hydrogen can be converted back into electricity using fuel cells or combustion engines, releasing only water vapour as a byproduct [226]. This makes green hydrogen a clean and efficient way to store and release

energy, aiding in the transition to a sustainable energy system. However, the efficiency of electricity-hydrogen is only 55–75% depending on the transformation method [232].

In Australia, the existing natural gas network can be supplemented with green hydrogen to reduce greenhouse gas emissions [226]. The injection of 2% hydrogen into the existing network has already been trialed and larger commercial gas turbines are capable of processing higher percentages of hydrogen (75%) [233]. However, the injection of 10% hydrogen into the existing gas network will require significant additional infrastructure and retrofitting of the network. The use of this technology is also complicated in remote areas of Australia which would require high capital investment. The Australian government has established a \$2 billion hydrogen head start initiative which aims to scale up large green hydrogen projects in Australia. However, the technology is still in its infancy in Australia [234].

5.5. Batteries

Batteries are the most used energy storage system globally. The earliest battery can be traced back to Bagdad, Iraq (Mesopotamia), and dates back over 2000 years ago. In 1938 archaeologists found jars composed of an iron rod in a copper cylinder with an asphalt stopper and it is believed that the Parthian civilisation used such jars to plate gold onto silver [235,236]. In 1800, Alessandro Volta demonstrated a device formed from an alternate stack of zinc and silver plates isolated from each other by a piece of cloth dipped in a solution of weak acid and salt. This was the first demonstration of what can be recognised as a modern battery [237].

Currently, battery application ranges from micro batteries measuring only 3 mm × 3 mm with a capacity of 2 mAh [238], to one of the most commonly used batteries in the world, the 18,560 cylindrical lithium-ion battery, measuring 18 mm by 65 mm with a capacity ranging from 1500 mAh to 3500 mAh for commercial batteries; in large-scale commercial applications, capacities are measured in MWh.

Batteries are used in everything from internal medical devices to personal devices such as watches and phones to electrical cars. Large-scale applications are used to store renewable energy storage such as the massive Edwards and Sanborn solar and energy storage system used in America, which has an impressive 3287 MWh capacity battery [239]. Batteries have become ubiquitous in most regions of the world, and battery technology has evolved for specific applications. The metal ion batteries, such as lithium and sodium ion batteries, have high power and energy density, comparatively long life, and high cycle efficiencies. Lithium-ion batteries have become very popular with the advancement of electrical vehicle usage and the advancements in technology that require high capacity but low-profile energy storage. As a result, the use of LiBs is expected to increase with the global demand of batteries expected to reach up to 130,000 GWh by 2040 if current trends are maintained [240]. As popular as LiBs are, there are several disadvantages. One of the largest of which is thermal runaway, which poses significant risks of fire and explosion. Numerous recent examples have linked LiB to fire outbreaks [241]. The Australia Fire and Rescue Services New South Wales, one of the world's largest urban fire and rescue services, reported that approximately 1 in every 100 fires attended by the department involved lithium ion batteries [242]. In addition, the complex battery construction complicates the recycling and recovery of the battery material, specifically the black mass. Currently, only 10% of discarded LiBs are recycled in Australia, raising concerns about the environmental impact of these batteries [243].

In contrast, older battery technologies such as lead acid (LA) batteries have comparatively reduced power and energy density (300 W/kg and 75 Wh/kg, respectively) and concerns have been raised about the environmental and health impacts of using lead

electrodes; however, the technology has several advantages [226]. LA batteries are sealed and spill-proof, can be operated at temperatures from -40°C to 55°C , and are easily recyclable with up to 99% recovery of the material [226,243]. The use of this technology is still common globally and remains one of the cheapest energy storage technologies.

Comparatively, RFBs offer several advantages, including scalability, a long cycle life, and the ability to independently size power and energy capacities. This makes them ideal for large-scale energy storage applications, such as balancing renewable energy sources and providing grid stability. They also have a relatively low environmental impact and can be recharged quickly. At larger capacities ($>8\text{ kWh}$), RFB costs are comparable with lithium iron phosphate batteries and are ideal for large-scale renewable energy storage [226,231]. A detailed overview of RFBs usage in Australia is provided below.

5.6. Redox Flow Batteries in Australia

RFBs have become significant due to their distinct characteristics and appropriateness for large-scale energy storage applications. RFBs present several economic benefits compared to other types of batteries, making them an appealing energy storage option in Australia, particularly in areas with high renewable energy generation.

Australia's substantial vanadium reserves make VRFBs attractive, spurring interest in developing a domestic RFB industry. These resources support Australia's goal of creating strong critical minerals supply chain for advanced technologies like batteries. Established in 2019, the Future Battery Industries Cooperative Research Centre (FBICRC) aims to promote innovation, research, and commercialisation of advanced battery technologies. It is a collaborative effort involving industry, government, and research institutions, enhancing Australia's position as a leader in battery development.

The following are some of the benefits of RFBs in the Australian context:

- Long Cycle Life: RFBs typically have long cycle lives, often exceeding 20,000 cycles [113], reducing the need for frequent replacements and lowering the overall cost of energy storage. In comparison, lithium batteries have a 3000-cycle lifespan at an 80% deep discharge [119]. VRFBs are suggested to be more efficient in hot climates, where lithium batteries age faster and incur higher long-term costs due to the increased temperatures [244].
- Scalability: RFBs are highly scalable, allowing users to adjust the system size to meet their specific energy storage needs by increasing the electrolyte volume. This flexibility can lead to cost savings by avoiding the over-sizing of storage systems [244].
- Low Maintenance: RFBs need less upkeep than many other energy storage technologies. Separating the electrolyte storage from the cell makes maintenance simpler, lowering operational costs.
- Safety: RFBs are regarded as safer because they use non-flammable and non-toxic electrolytes [245]. Compared to other battery types, RFBs present a lower risk of thermal runaway or fire incidents, which can pose significant hazards in certain scenarios [245–248].
- Environmental Impact: RFBs can be more environmentally friendly. For example, VRFBs use vanadium, which is relatively abundant and efficiently recyclable. In contrast, the recycling processes for other battery technologies, such as lithium batteries, pose higher risks, including an increased risk of combustion, greater environmental impact, and more complexity [249,250].

While RFBs offer these advantages, it is essential to note that the viability of the technology can vary depending on factors such as location, electricity prices, system size, and the specific application. A thorough economic analysis should be conducted to assess the financial feasibility of deploying RFBs in a particular context in Australia. Due to the

low rate of industrial application, the amount of information on costs of various RFBs are limited. However, recent work evaluated the commercial viability of existing RFB technologies to help guide research and development. It compared the levelised capital cost (LCOS) of storage for different RFBs to account for operating cost, capital cost, and energy throughput over the life of the project [251]. The results can be seen in Table 7. Although the LCOS for lithium iron phosphate is the lowest, it is also the most commercialised of the batteries, which helps decrease the associated costs. ZBRFB have not been included in the analysis; however, when integrated into a complete system, the cost is approximately \$200 kWh, comparable with that of VRFBs [51].

Table 7. Economic analysis of different battery types based on the power density and round-trip efficiency of each. Adapted from [251].

Battery Type	Round Trip Efficiency	Power Density (W/cm ²)	Reactor Cost (\$/kWh)	Chemical Costs (\$/kWh)	Capital Costs (\$/kWh)	LCOS (\$/MWh)	Capital Loss (%/Cycle)
Lithium iron phosphate	98	0.0032	-	101	101	64	0.067
Iron chromium	67	0.18	57	36	92	73	0.222
Polysulphide permanganate flow battery	50	0.08	199	7	206	130	0.015
All vanadium redox flow battery	81	0.3	33	140	173	98	0.171
Polysulphide ferricyanide redox flow battery	62	0.14	70	23	93	76	0.075
Polysulphide sodium/bromine redox flow battery	57	0.19	111	10	121	91	0.681

In Australia, various RFB systems with distinct chemistries have been implemented. Reflow, a company specialising in zinc-bromine batteries located in Queensland, Australia, has installed multiple systems. Energy Storage Industries has implemented iron flow systems and is currently constructing a factory for iron flow batteries in Queensland. The most extensively researched and well-documented RFB is the VRFB. Significant efforts have been devoted to understanding its electrochemical properties, and global initiatives are actively progressing towards its commercial utilisation. In Australia, several VRFB systems have been built and are currently operational, with additional projects in the planning stages (Figure 13, Table 8) [252].

Table 8. List of current and announced VRFB locations around Australia [252].

Map No.	Manufacturer	Organisation	Location	Power (kW)	Hours	Capacity (kWh)	Status
1	Shanghai Electric	Household VRFB Energy Storage Projects	Northern Territories	2.5	4	10	Operational
2	UET	University of Queensland	Heron Island, Queensland	125	5	625	Decommissioned
3	StorEn Technologies	StorEn-Multicom Resources Limited	Brisbane, Queensland	30			Speculative
4	CellCube	University of New South Wales	Sydney, New South Wales	30	4	129	Operational
5	CellCube	Auckland	Auckland, New South Wales	30	4	120	Operational
6	redT Energy	Monash University	Melbourne, Victoria	180	5	900	Operational
7	VSUN Energy	Priest Bros Orchard	Pakenham, Victoria	20	4	80	Announced
8	VSUN Energy	Meredith Dairy	Meredith, Victoria	80	4	320	Announced
9	UET	University of Adelaide—Roseworthy Solar Farm	Roseworthy, South Australia	100	4	400	Operational
10	VSUN Energy	University of Adelaide	Adelaide, South Australia	135	3.33	450	Under Construction
11	Invinity Energy Systems	Yadlamalka Energy Trust	Yadlamalka, South Australia	2000	4	8000	Operational
12	CellCube	CellCube Pangea	Port Augusta, South Australia	50,000	4	200,000	Announced
13	VSUN Energy	Busselton Farm Property	Busselton, Western Australia	10	10	100	Operational

Table 8. Cont.

Map No.	Manufacturer	Organisation	Location	Power (kW)	Hours	Capacity (kWh)	Status
14	Protean Energy	Ozline industries	Perth, Western Australia	5	20	100	Operational
15	VSUN Energy	Standalone EV Battery Charger Research Project	Bayswater, Western Australia	5	6	30	Trial Completed
16	Ultra Power Systems	Thorion Energy	Perth, Western Australia	6	6.6	40	Operational
17	Avess Energy	Avess energy group	Windimurra, Western Australia	50	5	250	Announced
18	VSun Energy	IGO	Fraser Range, Western Australia	50	6	300	Under construction
19	Invinity Energy Systems	VSUN Energy/Horizon Power	Kununurra, Western Australia	78	2.82	220	Pilot
20	VRB Energy	King Island Renewable Energy Expansion VRB	Currie, Tasmania	200	4	800	Decommissioned



Figure 13. A map of current and announced VRFB projects across Australia as of 2023 (adapted from [252]). The numbers in the image relate to Map. No.'s in Table 8.

Australia is well positioned to adopt VRFB technology. In 2022, about 32% of the nation's total energy production originated from renewable sources [253]. The Australian federal government has set a target of achieving 82% renewable energy by 2030 [254], creating a demand for energy storage solutions such as VRFBs. This supports the development of vanadium electrolyte production across Australia. The country possesses one of the world's largest vanadium reserves, accounting for 29% of global vanadium deposits [255] distributed nationwide (Figure 14). The largest deposits are in Western Australia, in which most of the geological region is Cenozoic. The majority of mining project in Western Australia focus on vanadium titanium magnetite. In Queensland, where the majority of the geological region is Mesozoic, mining operations are focused mostly on shale-hosted vanadium (Table 9).

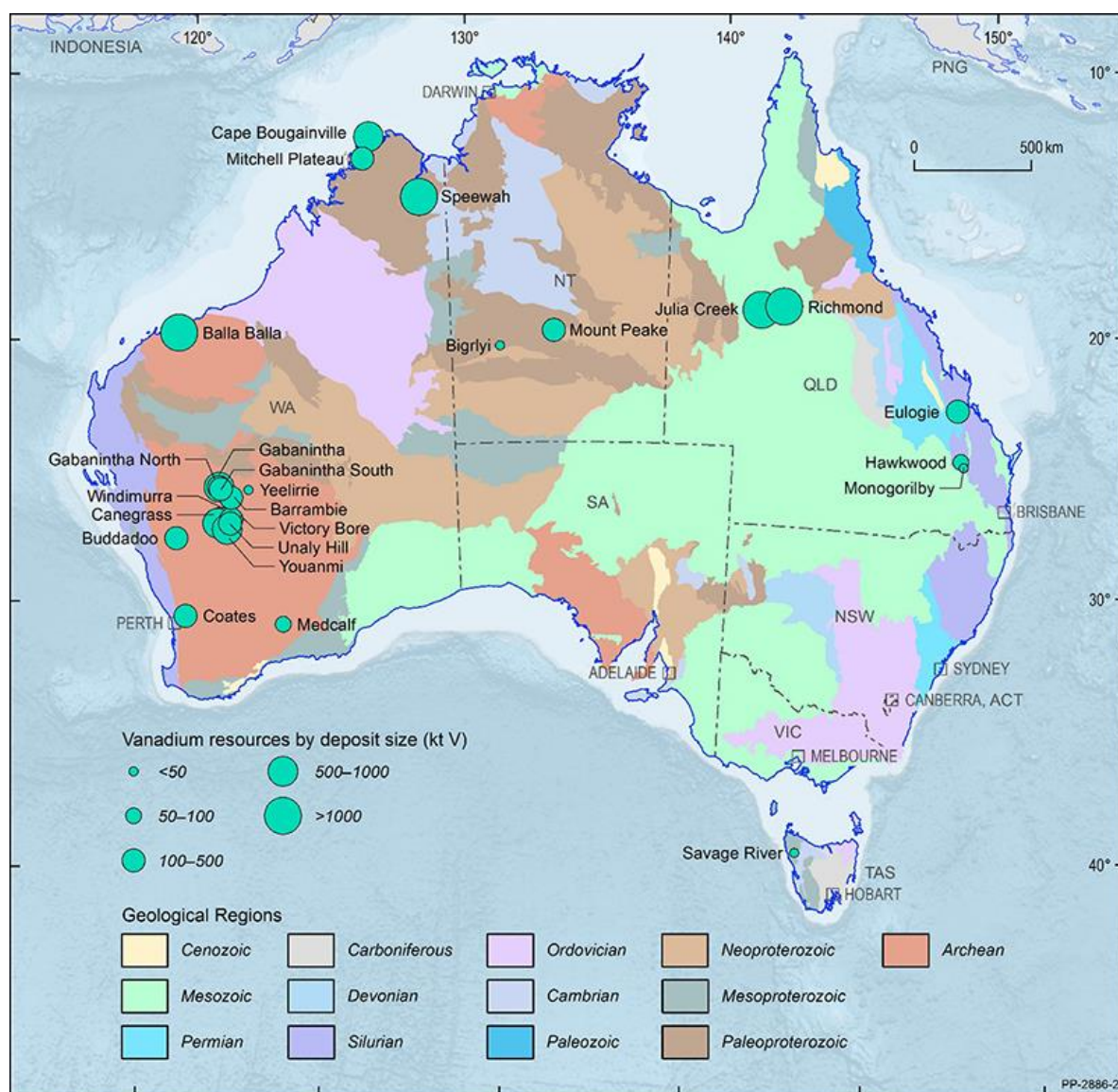


Figure 14. Map illustrating the known vanadium deposits and their estimated scale throughout Australia. The circles represent the vanadium deposit size in kiloton. The colours on the map are representative of various geological regions [253].

Table 9. List of current mining projects around Australia, the resource type mined, the resource output from the mining projects, and the state/territory in which the mining projects are located [252].

Project	Organisation	Resource Type	Resource Output	Location
Mount Peak	Tivan resources	VTM	VTMOC	Northern Territory
Vecco V + HPA project	Vecco group	SHV	BS-HVOO	Queensland
Saint Elmo	Mulitcom Resources Ltd.	SHV	CO	Queensland
Julia Creek project	Qem Ltd.	SHV	VBOS	Queensland
Toolebuc project	Toulebuc project	SHV	BS-HVOO	Queensland
The Richmond-Julia creek project	Richmond Vanadium Technology	SHV	BS-HVOO	Queensland
Speewah	Tivan Resources	VTM	VTMOC	Western Australia
Coates Project	Australian Vanadium limited	VTM	VTMOC	Western Australia
Buddadoo	Czr resources	VTM	VTMOC	Western Australia
Canegrass	Flinders mine Ltd.	VTM	VTMOC	Western Australia
Vindimurra project	Atlantic Ltd.	VTM	VTMOC	Western Australia

Table 9. Cont.

Project	Organisation	Resource Type	Resource Output	Location
Younami-V-Oxide	Venus metals corporation Ltd.	VTM	VTMOC	Western Australia
Victory Bore and Unaly hill projects	Surefire Resources NI	VTM	VTMOC	Western Australia
Barrambie	Neometals Ltd.	VTM	VTMOC	Western Australia
Gabanitha-Murchison Technology metals project		VTM	VTMOC	Western Australia
Yarrabubba-Murchison Technology metals project	Technology metals Australia Ltd.	VTM	VTMOC	Western Australia
Australian Vanadium Project	Australian Vanadium Ltd.	VTM	VTMOC	Western Australia
Nowthanna Hill	Australian Vanadium Ltd.	SHV	CO	Western Australia
Balla Balla	Forge metals Ltd.	VTM	VTMOC	Western Australia

VTM: Vanadium titanium magnetite, VTMOC: Vanadium titanium magnetite ore concentrate, SHV: Shale-hosted vanadium, BS-H VOO: Black shale hosted-vanadium oxide ore, CO: Carnotite ore, VBOS: Vanadium-bearing oil shale.

This abundance of resources, combined with favourable renewable energy generation conditions, presents a case for implementing VRFB technology nationwide. Currently, two companies, Vecco Group and Australian Vanadium (AVL), have established a vanadium electrolyte manufacturing plant in Australia, indicating a potential for further expansion [256].

Until recently, Redflow International Pty Ltd. (Brisbane, Australia) was the sole Australian company engaged in the development of zinc bromine batteries [257] after the ZBB Energy Corporation (EnSync Energy Systems) closure. However, the company ceased operation in 2024. The estimated gross installed capacities of zinc-based FB are 2.23 MWh for Redflow, 5.67 MWh for ZBB Energy Corp., and 327 MWh for Premium Power [186]. With Redflow's closure, there are no longer any companies in Australia producing zinc bromine batteries.

6. Conclusions

Redox flow batteries (RFBs) offer a promising solution for energy storage, particularly within the context of Australia's expanding renewable energy sector. Since the technology's inception in 1974, extensive research and development have led to many variations in the initial design, each with distinct advantages and limitations. These include classical or true RFBs, where all the components are in solution, as well as hybrid RFBs, which can be solid/liquid, semi-solid, or gas/liquid. The design of RFBs varies significantly due to the different electrolyte utilised. Collectively, RFB technologies present several advantages over other energy storage technologies, such as lithium batteries, owing to their ease of scalability, cost-effectiveness, long cycle life, and ease of integration into existing energy grids. These properties render RFBs an attractive option for renewable energy storage, especially in remote areas. While multiple companies have already commercialised this technology, further research is required to enhance the stability, longevity, and energy density of the electrolyte. The unique design of RFBs, which separates energy capacity and power, offers significant benefits in terms of scalability, modularity, and adaptability. Despite certain limitations, such as lower energy density and the potential use of expensive or scarce materials, the benefits of RFBs, including long cycle life, cost-effectiveness, and environmental sustainability, position them as a key technology for achieving net-zero emissions.

In Australia, the geographical distribution of the population and the increasing reliance on renewable energy sources like photovoltaic panels and wind turbines underscore the need for efficient and reliable energy storage systems. RFBs provide a locally tailored approach to energy storage, addressing the logistical and economic challenges of large central energy storage systems. The successful implementation of RFBs in Australia could serve as a model for other regions facing similar energy storage challenges. The continued development and deployment of RFB technology will be essential in supporting the transition to a more sustainable and resilient energy system in Australia and beyond.

Funding: This research was funded by the Australian Future Battery Industries Cooperative Research Centre (FBICRC) as part of the Commonwealth Cooperative Research Centre Program. The article was prepared as part of the FBICRC project No. 038, titled: ‘Vanadium Electrolyte Development’. The authors gratefully acknowledge the support of the FBI CRC and participant organisations.

Conflicts of Interest: The authors declare no conflict of interest.

References

1. Yang, Z.; Liu, J.; Baskaran, S.; Imhoff, C.H.; Holladay, J.D. Enabling Renewable Energy-and the Future Grid-with Advanced Electricity Storage. *JOM* **2010**, *62*, 14–23. [CrossRef]
2. Gajdzik, B.; Wolniak, R.; Nagaj, R.; Źuromskaitė-Nagaj, B.; Grebski, W.W. The Influence of the Global Energy Crisis on Energy Efficiency: A Comprehensive Analysis. *Energies* **2024**, *17*, 947. [CrossRef]
3. Nikoloski, A.; Issa, T.B. *Development of Electrolytes for Vanadium Redox Flow Batteries*; Future Battery Industries CRC: Bentley, Australia, 2023.
4. Martins, F.; Felgueiras, C.; Smitkova, M.; Caetano, N. Analysis of Fossil Fuel Energy Consumption and Environmental Impacts in European Countries. *Energies* **2019**, *12*, 964. [CrossRef]
5. Hai, T.; Ali, M.A.; Zeki, F.M.; Chauhan, B.S.; Metwally, A.S.M.; Ullah, M. Optimal design of inter-state hydrogen fuel cell vehicle fueling station with on-site hydrogen production. *Int. J. Hydrogen Energy* **2024**, *52*, 733–745. [CrossRef]
6. van den Bergh, J.C.J.M.; Botzen, W.J.W. Monetary valuation of the social cost of CO₂ emissions: A critical survey. *Ecol. Econ.* **2015**, *114*, 33–46. [CrossRef]
7. Khan, S.A.; Chakraborty, S.; Dash, K.K.; Dar, A.H.; Shawl, F.; Dash, S.K.; Singh, S.K.; Dwivedi, M.; Barik, D. Review of Solar Greenhouse Drying Systems in Conjunction with Hybrid Technological Features, Designs, Operations, and Economic Implications for Agro-Food Product Processing Application. *Energy Technol.* **2024**, *12*, 2400176. [CrossRef]
8. Houghton, J.T.; Jenkins, G.J.; Ephraums, J.J. *Climate Change: The IPCC Scientific Assessment*; Houghton, J.T., Jenkins, G.J., Ephraums, J.J., Eds.; The United Nations: New York, NY, USA, 1993.
9. Qiao, D.; Luo, Y.; Chu, Y.; Zhang, H.; Zhao, F. Decomposition of agriculture-related non-CO₂ greenhouse gas emissions in Chengdu: 1995–2020. *J. Clean. Prod.* **2024**, *434*, 140125. [CrossRef]
10. Boretti, A. Flow batteries for net zero in New Zealand. *Energy Storage* **2023**, *5*, e513. [CrossRef]
11. Gielen, D.; Boshell, F.; Saygin, D.; Bazilian, M.D.; Wagner, N.; Gorini, R. The role of renewable energy in the global energy transformation. *Energy Strategy Rev.* **2019**, *24*, 38–50. [CrossRef]
12. Kiasari, M.; Ghaffari, M.; Aly, H. A Comprehensive Review of the Current Status of Smart Grid Technologies for Renewable Energies Integration and Future Trends: The Role of Machine Learning and Energy Storage Systems. *Energies* **2024**, *17*, 4128. [CrossRef]
13. REN21. Renewables 2022 Global Status Report. 2022. Available online: <https://www.ren21.net/gsr-2022/> (accessed on 5 September 2023).
14. REN21. *Renewables 2024 Global Status: Report Collection, Global Overview*; Secretariat, R., Ed.; REN21: Paris, France, 2024.
15. Australian Department of Climate Change, Energy, the Environment and Water. Solar PV and Batteries. 2023. Available online: <https://www.energy.gov.au/households/solar-pv-and-batteries#:~:text=Australia> (accessed on 5 September 2023).
16. Root, C.; Presume, H.; Proudfoot, D.; Willis, L.; Masiello, R. Using battery energy storage to reduce renewable resource curtailment. In *IEEE Power & Energy Society Innovative Smart Grid Technologies Conference (ISGT)*; IEEE: Washington, DC, USA, 2017; pp. 1–5.
17. Saka, S. An Overview of Large-Scale Energy Storage Systems. In *Advanced Redox Flow Technology*; John Wiley & Sons, Inc.: Hoboken, NJ, USA, 2024; pp. 199–243.
18. National Research Council. *The National Academies Summit on America’s Energy Future: Summary of a Meeting*; The National Academies Press: Washington, DC, USA, 2008.
19. Muzammal Islam, M.; Yu, T.; Giannoccaro, G.; Mi, Y.; la Scala, M.; Nasab, M.R.; Wang, J. Improving Reliability and Stability of the Power Systems: A Comprehensive Review on the Role of Energy Storage Systems to Enhance Flexibility. *IEEE Access* **2024**, *12*, 152738–152765. [CrossRef]
20. Patrick, A.; Thompson, B. WA pays business to consume power. In *The Australian Financial Review*; Fairfax Media Publications Pty Limited: Melbourne, Australia, 2020.
21. Falope, T.; Lao, L.; Hanak, D.; Huo, D. Hybrid energy system integration and management for solar energy: A review. *Energy Convers. Manag.* **2024**, *21*, 100527. [CrossRef]
22. Breeze, P. *Power System Energy Storage Technologies*; Elsevier Science: Amsterdam, The Netherlands, 2018.
23. Shahzad, S.; Abbasi, M.A.; Shahid, M.B.; Guerrero, J.M. Unlocking the potential of long-duration energy storage: Pathways to net-zero emissions through global innovation and collaboration. *J. Energy Storage* **2024**, *97*, 112904. [CrossRef]

24. Servin-Balderas, I.; Wetser, K.; Heijne, A.T.; Buisman, C.; Hamelers, B. CO₂-based methane: An overlooked solution for the energy transition. *Energy Sustain. Soc.* **2024**, *14*, 57. [CrossRef]
25. Zhu, D.; Wang, Y.; Yue, S.; Xie, Q.; Pedram, M.; Chang, N. Maximizing return on investment of a grid-connected hybrid electrical energy storage system. In Proceedings of the 2013 18th Asia and South Pacific Design Automation Conference (ASP-DAC), Yokohama, Japan, 22–25 January 2013.
26. Abdi, H.; Mohammadi-ivatloo, B.; Javadi, S.; Khodaei, A.R.; Dehnavi, E. Energy storage systems. In *Distributed Generation Systems*; Gharehpetian, G.B., Agah, M.M., Eds.; Elsevier Inc.: Amsterdam, The Netherlands, 2017; pp. 333–368.
27. Metals, T. *TMT Key Investor in Future Battery Industries CRC's Electrolyte Project*; Technology Metals Australia Limited: Subiaco, Australia, 2022.
28. Rogers, C. Is It Time to Go with the Flow? 2020. Available online: <https://www.greenrecruitmentcompany.com/blog/2020/09/is-it-time-to-go-with-the-flow?source=google.com.au> (accessed on 13 February 2025).
29. Cipriano, G. Meeting Long Duration Storage Needs with Flow Batteries. In Proceedings of the New Energy Solutions Conference, Phoenix, AZ, USA, 25–28 June 2019.
30. Vorrath, S. Australia's first grid-scale vanadium flow battery to be built in South Australia. In *Renew Economy (Clean Energy News and Analysis)*; RenewEconomy.com.au: Mullumbimby, Australia, 2020.
31. Yadlamalka Energy. The Project, Detailed Summary of the Yadlamalka Energy Project. 2020. Available online: <https://yadlamalkaenergy.com/project/> (accessed on 15 December 2020).
32. Palamara, F. What the vanadium? *Aust. Paydirt* **2023**, *1*, 98–103.
33. Australian Trade and Investment Commission. New Vanadium Battery Powers Solar Grid Rollouts. 2023. Available online: <https://international.austrade.gov.au/en/news-and-analysis/success-stories/new-vanadium-battery-powers-solar-grid-rollouts> (accessed on 22 January 2025).
34. Chen, H.; Zhang, X.; Wu, S.; Chen, F.; Xu, J. A comparative study of iron-vanadium and all-vanadium flow battery for large scale energy storage. *Chem. Eng. J.* **2022**, *429*, 132403. [CrossRef]
35. Huang, Z.; Mu, A.; Wu, L.; Wang, H. Vanadium redox flow batteries: Flow field design and flow rate optimization. *J. Energy Storage* **2022**, *45*, 103526. [CrossRef]
36. Western Australian Government. *Long-Duration Storage Trial Securing Regional WA's Energy Future*; Western Australian Government: Perth, Australia, 2024.
37. Renard, C. *Les Piles Légères (Piles Chlorochromiques) du Ballon Dirigeable "La France"*; Masson: Issy-les-Moulineaux, France, 1890.
38. Kangro, W.; Pieper, H. Zur frage der speicherung von elektrischer energie in flüssigkeiten. *Electrochim. Acta* **1962**, *7*, 435–448. [CrossRef]
39. Kangro, W. Verfahren zur Speicherung von Elektrischer Energie. German Patent EP2853728B1, 23 September 2015.
40. Thaller, L.H. *Electrically Rechargeable Redox Flow Cells*, NASA TM X-71540; National Aeronautics and Space Administration: Washington, DC, USA, 1974.
41. Clemente, A.; Costa-Castelló, R. Redox Flow Batteries: A Literature Review Oriented to Automatic Control. *Energies* **2020**, *13*, 4514. [CrossRef]
42. Weber, A.Z.; Mench, M.M.; Meyers, J.P.; Ross, P.N.; Gostick, J.T.; Liu, Q. Redox flow batteries: A review. *J. Appl. Electrochem.* **2011**, *41*, 1137–1164. [CrossRef]
43. Walsh, F.C. Electrochemical technology for environmental treatment and clean energy conversion. *Pure Appl. Chem.* **2001**, *73*, 1819–1837. [CrossRef]
44. Price, A.; Bartley, S.; Male, S.; Cooley, G. A novel approach to utility-scale energy storage. *Power Eng. J.* **1999**, *13*, 122–129. [CrossRef]
45. Skyllas-Kazacos, M.; Rychcik, M.; Robins, R.G.; Fane, A.G.; Green, M.A. New All-Vanadium Redox Flow Cell. *J. Electrochem. Soc.* **1986**, *133*, 1057–1058. [CrossRef]
46. Jonshagen, B.; James, G.; Issa, T.B. Report on ZBB/CSIRO Building energy Storage Project. In Proceedings of the International Flow Battery Forum (IFBF), Edinburgh, UK, 25–27 November 2011.
47. Jonshagen, B.; Issa, T.B. Zinc Bromine Flow Battery. In Proceedings of the First International Flow Battery Forum (IFBF), Vienna, Austria, 13 November 2010.
48. Singh, P.; Jonshagen, B. Zinc-bromine battery for energy storage. *J. Power Sources* **1991**, *35*, 405–410. [CrossRef]
49. Singh, P.; Jonshagen, B. Development of zinc-bromine battery. *Bull. Electrochem.* **1990**, *6*, 251–254.
50. Jimenez-Blasco, U.; Arrebola, J.C.; Caballero, A. Recent Advances in Bromine Complexing Agents for Zinc-Bromine Redox Flow Batteries. *Materials* **2023**, *16*, 7482. [CrossRef]
51. Alghamdi, N.S.; Rana, M.; Peng, X.; Huang, Y.; Lee, J.; Hou, J.; Gentle, I.R.; Wang, L.; Luo, B. Zinc-Bromine Rechargeable Batteries: From Device Configuration, Electrochemistry, Material to Performance Evaluation. *Nano-Micro Lett.* **2023**, *15*, 209. [CrossRef]
52. Arenas, L.F.; de León, C.P.; Walsh, F.C. Engineering aspects of the design, construction and performance of modular redox flow batteries for energy storage. *J. Energy Storage* **2017**, *11*, 119–153. [CrossRef]

53. Skyllas-Kazacos, M.; Chakrabarti, M.H.; Hajimolana, S.A.; Mjalli, F.S.; Saleem, M. Progress in Flow Battery Research and Development. *J. Electrochem. Soc.* **2011**, *158*, R55. [[CrossRef](#)]
54. Krishan, O.; Suhag, S. An updated review of energy storage systems: Classification and applications in distributed generation power systems incorporating renewable energy resources. *Int. J. Energy Res.* **2019**, *43*, 6171–6210. [[CrossRef](#)]
55. Alotto, P.; Guarneri, M.; Moro, F. Redox flow batteries for the storage of renewable energy: A review. *Renew. Sustain. Energy Rev.* **2014**, *29*, 325–335. [[CrossRef](#)]
56. Ressel, S.; Kuhn, P.; Fischer, S.; Jeske, M.; Struckmann, T. An all-extruded tubular vanadium redox flow cell—Characterization and model-based evaluation. *J. Power Sources Adv.* **2021**, *12*, 100077. [[CrossRef](#)]
57. Lucas, A.; Chondrogiannis, S. Smart grid energy storage controller for frequency regulation and peak shaving, using a vanadium redox flow battery. *Int. J. Electr. Power Energy Syst.* **2016**, *80*, 26–36. [[CrossRef](#)]
58. Girschik, J.; Kopietz, L.; Joemann, M.; Grevé, A.; Doetsch, C. Redox Flow Batteries: Stationary Energy Storages with Potential. *Chem. Ing. Tech.* **2021**, *93*, 523–533. [[CrossRef](#)]
59. Noack, J.; Roznyatovskaya, N.; Herr, T.; Fischer, P. The Chemistry of Redox-Flow Batteries. *Angew Chem. Int. Ed. Engl.* **2015**, *54*, 9776–9809. [[CrossRef](#)]
60. Zeng, Y.K.; Zhao, T.S.; An, L.; Zhou, X.L.; Wei, L. A comparative study of all-vanadium and iron-chromium redox flow batteries for large-scale energy storage. *J. Power Sources* **2015**, *300*, 438–443. [[CrossRef](#)]
61. Winardi, S.; Poon, G.; Ulaganathan, M.; Parasuraman, A.; Yan, Q.; Wai, N.; Lim, T.M.; Skyllas-Kazacos, M. Effect of Bromine Complexing Agents on the Performance of Cation Exchange Membranes in Second-Generation Vanadium Bromide Battery. *ChemPlusChem* **2015**, *80*, 376–381. [[CrossRef](#)]
62. Poon, G.; Parasuraman, A.; Lim, T.M.; Skyllas-Kazacos, M. Evaluation of N-ethyl-N-methyl-morpholinium bromide and N-ethyl-N-methyl-pyrrolidinium bromide as bromine complexing agents in vanadium bromide redox flow batteries. *Electrochim. Acta* **2013**, *107*, 388–396. [[CrossRef](#)]
63. Rui, X.; Oo, M.O.; Sim, D.H.; Raghu, S.C.; Yan, Q.; Lim, T.M.; Skyllas-Kazacos, M. Graphene oxide nanosheets/polymer binders as superior electrocatalytic materials for vanadium bromide redox flow batteries. *Electrochim. Acta* **2012**, *85*, 175–181. [[CrossRef](#)]
64. Prifti, H. Electrolyte and membrane studies of the novel vanadium bromide redox flow cell. In *Chemical Sciences & Engineering, Faculty of Engineering*; The University of New South Wales: Sydney, Australia, 2008.
65. Poon, G. Bromine Complexing Agents For Use in Vanadium Bromide (V/Br) Redox Flow Cell. In *School of Chemical Sciences and Engineering*; The University of New South Wales: Sydney, Australia, 2008.
66. Skyllas-Kazacos, M.; Limantari, Y. Kinetics of the chemical dissolution of vanadium pentoxide in acidic bromide solutions. *J. Appl. Electrochem.* **2004**, *34*, 681–685. [[CrossRef](#)]
67. Ma, Q.; Xing, L.; Li, H.; Leung, P.; Yang, W.; Su, H.; Xu, Q. Modeling the effect of temperature on performance of an iron-vanadium redox flow battery with deep eutectic solvent (DES) electrolyte. *J. Power Sources* **2020**, *449*, 227491.
68. Xu, J.; Ma, Q.; Zhao, L.; Xu, J.; Su, H.; Zhang, W.; Yang, W.; Xu, Q. Pore-scale investigation of reactive transfer process in a deep eutectic solvent (DES) electrolyte-based vanadium-iron redox flow battery. *Electrochim. Acta* **2020**, *353*, 136486.
69. Souentie, S.; Amr, I.; Alsuhailani, A.; Almazroei, E.; Hammad, A.D. Temperature, charging current and state of charge effects on iron-vanadium flow batteries operation. *Appl. Energy* **2017**, *206*, 568–576. [[CrossRef](#)]
70. Xue, F.-Q.; Wang, Y.-L.; Wang, W.-H.; Wang, X.-D. Investigation on the electrode process of the Mn(II)/Mn(III) couple in redox flow battery. *Electrochim. Acta* **2008**, *53*, 6636–6642. [[CrossRef](#)]
71. Reynard, D.; Girault, H. Combined hydrogen production and electricity storage using a vanadium-manganese redox dual-flow battery. *Cell Rep. Phys. Sci.* **2021**, *2*, 100556. [[CrossRef](#)]
72. Reynard, D.; Maye, S.; Peljo, P.; Chanda, V.; Girault, H.H.; Gentil, S. Vanadium-Manganese Redox Flow Battery: Study of Mn(III) Disproportionation in the Presence of Other Metallic Ions. *Chemistry* **2020**, *26*, 7250–7257. [[CrossRef](#)]
73. Yun, S.; Parrondo, J.; Ramani, V. A Vanadium-Cerium Redox Flow Battery with an Anion-Exchange Membrane Separator. *ChemPlusChem* **2015**, *80*, 412–421. [[CrossRef](#)]
74. Leung, P.K.; Mohamed, M.R.; Shah, A.A.; Xu, Q.; Conde-Duran, M.B. A mixed acid based vanadium–cerium redox flow battery with a zero-gap serpentine architecture. *J. Power Sources* **2015**, *274*, 651–658. [[CrossRef](#)]
75. Govindan, M.; He, K.; Moon, I.-S. Evaluation of Dual Electrochemical Cell Design for Cerium-Vanadium Redox Flow Battery to Use Different Combination of Electrodes. *Int. J. Electrochem. Sci.* **2013**, *8*, 10265–10279. [[CrossRef](#)]
76. Liu, Y.; Xia, X.; Liu, H. Studies on cerium ($\text{Ce}^{4+}/\text{Ce}^{3+}$)–vanadium($\text{V}^{2+}/\text{V}^{3+}$) redox flow cell—Cyclic voltammogram response of $\text{Ce}^{4+}/\text{Ce}^{3+}$ redox couple in H_2SO_4 solution. *J. Power Sources* **2004**, *130*, 299–305. [[CrossRef](#)]
77. Xia, X.; Liu, H.-T.; Liu, Y. Studies of the Feasibility of a $\text{Ce}^{4+}/\text{Ce}^{3+}-\text{V}^{2+}/\text{V}^{3+}$ Redox Cell. *J. Electrochem. Soc.* **2002**, *149*, A426. [[CrossRef](#)]
78. Paulenovaa, A.; Creager, S.E.; Navratila, J.D.; Weic, Y. Redox potentials and kinetics of the $\text{Ce}^{3+}/\text{Ce}^{4+}$ redox reaction and solubility of cerium sulfates in sulfuric acid solutions. *J. Power Sources* **2002**, *109*, 431–438. [[CrossRef](#)]

79. Fang, B.; Iwasa, S.; Wei, Y.; Arai, T.; Kumagai, M. A study of the Ce(III)/Ce(IV) redox couple for redox flow battery application. *Electrochim. Acta* **2002**, *47*, 3971–3976. [CrossRef]
80. Zhang, Q.; Jiang, H.; Liu, S.; Wang, Q.; Wang, J.; Zhou, Z.; Cai, K.; Lai, Q.; Wang, Q. Redox-targeting catalyst developing new reaction path for high-power zinc-bromine flow batteries. *J. Power Sources* **2024**, *601*, 234286. [CrossRef]
81. Sun, X.; Wang, D.; Hu, H.; Wei, X.; Meng, L.; Ren, Z.; Li, S. Double-Doped Carbon-Based Electrodes with Nitrogen and Oxygen to Boost the Areal Capacity of Zinc-Bromine Flow Batteries. *Trans. Tianjin Univ.* **2024**, *30*, 74–89. [CrossRef]
82. Jin, C.-X.; Lei, H.-Y.; Liu, M.-Y.; Tan, A.-D.; Piao, J.-H.; Fu, Z.-Y.; Liang, Z.-X.; Wang, H.-H. Low-dimensional nitrogen-doped carbon for Br₂/Br⁻ redox reaction in zinc-bromine flow battery. *Chem. Eng. J.* **2020**, *380*, 122606. [CrossRef]
83. Wu, M.; Zhao, T.; Wei, L.; Jiang, H.; Zhang, R. Improved electrolyte for zinc-bromine flow batteries. *J. Power Sources* **2018**, *384*, 232–239. [CrossRef]
84. Singh, P.; White, K.; Parker, A.J. Application of non-aqueous solvents to batteries part I. Physicochemical properties of propionitrile/water two-phase solvent relevant to zinc—Bromine. *J. Power Sources* **1983**, *10*, 309–318. [CrossRef]
85. Bajpai, S.N. Vapor pressures of bromine-quaternary ammonium salt complexes for zinc-bromine battery applications. *J. Chem. Eng. Data* **1981**, *26*, 2–4. [CrossRef]
86. Ponce de León, C.; Frías-Ferrer, A.; González-García, J.; Szánto, D.A.; Walsh, F.C. Redox flow cells for energy conversion. *J. Power Sources* **2006**, *160*, 716–732. [CrossRef]
87. Blackridge Research & Consulting. Here's the Top 10 List of Flow Battery Companies. 2022. Available online: <https://www.blackridgeresearch.com/blog/top-flow-battery-companies-manufacturers> (accessed on 3 August 2022).
88. Zhao, X.; Kim, Y.-B.; Jung, S. Shunt current analysis of vanadium redox flow battery system with multi-stack connections. *J. Energy Storage* **2023**, *73*, 109233. [CrossRef]
89. Sun, C.; Negro, E.; Nale, A.; Pagot, G.; Vezzù, K.; Zawodzinski, T.A.; Meda, L.; Gambaro, C.; Di Noto, V. An efficient barrier toward vanadium crossover in redox flow batteries: The bilayer [Nafion/(WO₃)_x] hybrid inorganic-organic membrane. *Electrochim. Acta* **2021**, *378*, 138133. [CrossRef]
90. Wu, X.; Hu, J.; Liu, J.; Zhou, Q.; Zhou, W.; Li, H.; Wu, Y. Ion exchange membranes for vanadium redox flow batteries. *Pure Appl. Chem.* **2014**, *86*, 633–649. [CrossRef]
91. Sinclair, N.; Vasil, M.; Kellamis, C.; Nagelli, E.A.; Wainright, J.; Savinell, R.; Wnek, G.E. Membrane Considerations for the All-Iron Hybrid Flow Battery. *J. Electrochem. Soc.* **2023**, *170*, 050516. [CrossRef]
92. Ye, Z.; Chen, N.; Zheng, Z.; Xiong, L.; Chen, D. Preparation of Sulfonated Poly(arylene ether)/SiO(2) Composite Membranes with Enhanced Proton Selectivity for Vanadium Redox Flow Batteries. *Molecules* **2023**, *28*, 3130. [CrossRef]
93. Oei, D.-G. Permeation of vanadium cations through anionic and cationic membranes. *J. Appl. Electrochem.* **1985**, *15*, 231–235. [CrossRef]
94. Berezina, N.P.; Kononenko, N.A.; Dyomina, O.A.; Gnusin, N.P. Characterization of ion-exchange membrane materials: Properties vs structure. *Adv Colloid Interface Sci* **2008**, *139*, 3–28. [CrossRef]
95. Li, J.; Xu, F.; Chen, W.; Han, Y.; Lin, B. Anion Exchange Membranes Based on Bis-Imidazolium and Imidazolium-Functionalized Poly(phenylene oxide) for Vanadium Redox Flow Battery Applications. *ACS Omega* **2023**, *8*, 16506–16512. [CrossRef]
96. Krowne, C.M. Measures of Performance of Vanadium and Other Redox Flow Batteries. *J. Electrochem. Soc.* **2024**, *171*, 050538. [CrossRef]
97. Sánchez-Díez, E.; Ventosa, E.; Guarnieri, M.; Trovò, A.; Flox, C.; Marcilla, R.; Soavi, F.; Mazur, P.; Aranzabe, E.; Ferret, R. Redox flow batteries: Status and perspective towards sustainable stationary energy storage. *J. Power Sources* **2021**, *481*, 228804. [CrossRef]
98. Pissoort, P.A. Storage Batteries. FR 754065, 30 October 1933.
99. Pelligri, A.; Spaziente, P.M. Process and Accumulator for Storing and Releasing Electrical Energy. GB Patent 2030349, 28 July 1982.
100. Skyllas-Kazacos, M.; Rychick, M.; Robins, R. All-Vanadium Redox Battery. US4786567, 22 November 1988.
101. Iwakiri, I.; Antunes, T.; Almeida, H.; Sousa, J.P.; Figueira, R.B.; Mendes, A. Redox Flow Batteries: Materials, Design and Prospects. *Energies* **2021**, *14*, 5643. [CrossRef]
102. García-Limón, B.Y.; Salazar-Gastélum, L.J.; Salazar-Gastélum, M.I.; Lin, S.W.; Calva-Yáñez, J.C.; Beltrán-Gastelum, M.; Zizumbo-López, A.; Pérez-Sicairos, S. Composite Membranes of PVDF/PES/SPEES for Flow Battery Applications. *J. Electron. Mater.* **2024**, *53*, 3289–3299. [CrossRef]
103. Sharma, J.; Kulshrestha, V. Advancements in polyelectrolyte membrane designs for vanadium redox flow battery (VRFB). *Results Chem.* **2023**, *5*, 100892. [CrossRef]
104. Puleston, T.; Cecilia, A.; Costa-Castelló, R.; Serra, M. Vanadium redox flow batteries real-time State of Charge and State of Health estimation under electrolyte imbalance condition. *J. Energy Storage* **2023**, *68*, 107666. [CrossRef]
105. Skyllas-Kazacos, M.; McCann, J.F. Chapter 10—Vanadium redox flow batteries (VRBs) for medium- and large-scale energy storage. In *Advances in Batteries for Medium and Large-Scale Energy Storage*; Menictas, C., Skyllas-Kazacos, M., Lim, T.M., Eds.; Woodhead Publishing: London, UK, 2015; pp. 329–386.

106. Krown, C.M. Determination of the Ion Concentrations in VRFB by Non-Invasive Optical Techniques Due to Chemical Reactions, Complexes, and Side Reactions. *J. Electrochem. Soc.* **2024**, *171*, 020546. [[CrossRef](#)]
107. Hagg, C.M.; Skyllas-Kazacos, M. Novel bipolar electrodes for battery applications. *J. Appl. Electrochem.* **2002**, *32*, 1063–1069. [[CrossRef](#)]
108. Ye, M.; Zhang, N.; Zhou, T.; Wei, Z.; Jiang, F.; Ke, Y. Recent research on vanadium redox batteries: A review on electrolyte preparation, mass transfer, and charge transfer for electrolyte performance enhancement. *Energy Storage* **2024**, *6*, e610. [[CrossRef](#)]
109. Parasuraman, A.; Lim, T.M.; Menictas, C.; Skyllas-Kazacos, M. Review of material research and development for vanadium redox flow battery applications. *Electrochim. Acta* **2013**, *101*, 27–40. [[CrossRef](#)]
110. Zarei-Jelyani, M.; Loghavi, M.M.; Babaiee, M.; Eqra, R. Comparative analysis of single-acid and mixed-acid systems as supporting electrolyte for vanadium redox flow battery. *J. Appl. Electrochem.* **2023**, *54*, 719–730. [[CrossRef](#)]
111. Jirabovornwisut, T.; Arpornwichanop, A. A review on the electrolyte imbalance in vanadium redox flow batteries. *Int. J. Hydrogen Energy* **2019**, *44*, 24485–24509. [[CrossRef](#)]
112. Skyllas-Kazacos, M.; Menictas, C. Vanadium Redox Flow Batteries. In *Encyclopedia of Energy Storage*; Elsevier: Amsterdam, The Netherlands, 2022; pp. 407–422.
113. Jiang, H.R.; Sun, J.; Wei, L.; Wu, M.C.; Shyy, W.; Zhao, T.S. A high power density and long cycle life vanadium redox flow battery. *Energy Storage Mater.* **2020**, *24*, 529–540. [[CrossRef](#)]
114. Kapoor, M.; Beriwal, N.; Verma, A. Maximizing durability of vanadium redox flow battery by evaluating electrolyte-repair-point. *J. Energy Storage* **2020**, *32*, 101759. [[CrossRef](#)]
115. Ra, N.; Dutta, A.; Bhattacharjee, A. Optimizing vanadium redox flow battery system power loss using particle swarm optimization technique under different operating conditions. *Int. J. Energy Res.* **2022**, *46*, 17346–17361. [[CrossRef](#)]
116. Wang, Y.; Mu, A.; Wang, W.; Yang, B.; Wang, J. A Review of Capacity Decay Studies of All-vanadium Redox Flow Batteries: Mechanism and State Estimation. *ChemSusChem* **2024**, *17*, e202301787. [[CrossRef](#)]
117. Skyllas-Kazacos, M. Review—Highlights of UNSW All-Vanadium Redox Battery Development: 1983 to Present. *J. Electrochem. Soc.* **2022**, *169*, 070513. [[CrossRef](#)]
118. Kapoor, M.; Verma, A. Technical benchmarking and challenges of kilowatt scale vanadium redox flow battery. *WIREs Energy Environ.* **2022**, *11*, e439. [[CrossRef](#)]
119. Doetsch, C.; Burfeind, J. Chapter 17: Vanadium Redox Flow Batteries. In *Storing Energy*; Letcher, T.M., Ed.; Elsevier: Oxford, UK, 2022; pp. 363–381.
120. Luo, X.; Wang, J.; Dooner, M.; Clarke, J. Overview of current development in electrical energy storage technologies and the application potential in power system operation. *Appl. Energy* **2015**, *137*, 511–536. [[CrossRef](#)]
121. Eckroad, S.; Gyuk, I. *EPRI-DOE Handbook of Energy Storage for Transmission & Distribution Applications*; Electric Power Research Institute, Inc.: Washington, DC, USA, 2003; pp. 3–35.
122. Hennessy; Kuntz. Flow Battery Storage Application with Wind Power. In Proceedings of the 2005/2006 IEEE/PES Transmission and Distribution Conference and Exhibition, Dallas, TX, USA, 21–24 May 2006.
123. Shigematsu, T.; Kumamoto, T.; Deguchi, H.; Hara, T. Applications of a vanadium redox-flow battery to maintain power quality. In Proceedings of the IEEE/PES Transmission and Distribution Conference and Exhibition, Yokohama, Japan, 6–10 October 2002.
124. Shibata, A.; Sato, K. Development of vanadium redox flow battery for electricity storage. *Power Eng. J.* **1999**, *13*, 130–135. [[CrossRef](#)]
125. Nimat, S.; Sarah, S.A.; Stephen, B.B. Renewable Energy Based Grid Connected Battery Projects around the World—An Overview. *J. Energy Power Eng.* **2019**, *13*, 1–23.
126. Kim, K.J.; Park, M.-S.; Kim, Y.-J.; Kim, J.H.; Dou, S.X.; Skyllas-Kazacos, M. A technology review of electrodes and reaction mechanisms in vanadium redox flow batteries. *J. Mater. Chem. A* **2015**, *3*, 16913–16933. [[CrossRef](#)]
127. Wei, X.; Liu, S.; Wang, J.; He, Z.; Zhao, K.; Yang, Y.; Liu, B.; Huang, R.; He, Z. Boosting the performance of positive electrolyte for VRFB by employing zwitterion molecule containing sulfonic and pyridine groups as the additive. *Ionics* **2020**, *26*, 3147–3159. [[CrossRef](#)]
128. Cao, L.; Skyllas-Kazacos, M.; Menictas, C.; Noack, J. A review of electrolyte additives and impurities in vanadium redox flow batteries. *J. Energy Chem.* **2018**, *27*, 1269–1291. [[CrossRef](#)]
129. Wu, X.; Liu, S.; Wang, N.; Peng, S.; He, Z. Influence of organic additives on electrochemical properties of the positive electrolyte for all-vanadium redox flow battery. *Electrochim. Acta* **2012**, *78*, 475–482. [[CrossRef](#)]
130. Lei, Y.; Liu, S.-Q.; Gao, C.; Liang, X.-X.; He, Z.-X.; Deng, Y.-H.; He, Z. Effect of Amino Acid Additives on the Positive Electrolyte of Vanadium Redox Flow Batteries. *J. Electrochem. Soc.* **2013**, *160*, A722–A727. [[CrossRef](#)]
131. Peng, S.; Wang, N.; Gao, C.; Lei, Y.; Liang, X.; Liu, S.; Liu, Y. Influence of trishydroxymethyl aminomethane as a positive electrolyte additive on performance of vanadium redox flow battery. *Int. J. Electrochem. Sci.* **2012**, *7*, 4314–4321. [[CrossRef](#)]
132. Leung, P.; Li, X.; de León, C.P.; Berlouis, L.; Low, C.T.J.; Walsh, F.C. Progress in redox flow batteries, remaining challenges and their applications in energy storage. *RSC Adv.* **2012**, *2*, 10125–10156. [[CrossRef](#)]

133. Zhang, Z.H.; Wei, L.; Wu, M.C.; Bai, B.F.; Zhao, T.S. Chloride ions as an electrolyte additive for high performance vanadium redox flow batteries. *Appl. Energy* **2021**, *289*, 116690. [[CrossRef](#)]
134. Nguyen, T.D.; Whitehead, A.; Wai, N.; Scherer, G.G.; Simonov, A.N.; Xu, Z.J.; MacFarlane, D.R. Advanced Electrolyte Formula for Robust Operation of Vanadium Redox Flow Batteries at Elevated Temperatures. *Small* **2024**, *20*, 2311771. [[CrossRef](#)]
135. Kim, G.; Kim, Y.; Yim, T.; Kwon, K. Effects of methanesulfonic acid on electrolyte for vanadium redox flow batteries. *J. Ind. Eng. Chem.* **2021**, *99*, 326–333. [[CrossRef](#)]
136. Wei, X.; Wang, G.; Li, F.; Zhang, J.; Chen, J.; Wang, R. High performance positive electrolyte with potassium diformate (KDF) additive for vanadium redox flow batteries. *Int. J. Electrochem. Sci.* **2022**, *17*, 220126. [[CrossRef](#)]
137. Yu, L.; Lin, F.; Xu, L.; Xi, J. A recast Nafion/graphene oxide composite membrane for advanced vanadium redox flow batteries. *Rsc Adv.* **2016**, *6*, 3756–3763. [[CrossRef](#)]
138. Wu, C.; Lu, S.; Zhang, J.; Xiang, Y. Inducing microstructural changes in Nafion by incorporating graphitic carbon nitride to enhance the vanadium-blocking effect. *Phys. Chem. Chem. Phys.* **2018**, *20*, 7694–7700. [[CrossRef](#)] [[PubMed](#)]
139. Chen, S.; Sun, C.; Zhang, H.; Yu, H.; Wang, W. Electrochemical Deposition of Bismuth on Graphite Felt Electrodes: Influence on Negative Half-Cell Reactions in Vanadium Redox Flow Batteries. *Appl. Sci.* **2024**, *14*, 3316. [[CrossRef](#)]
140. Mazúr, P.; Mrník, J.; Beneš, J.; Počedič, J.; Vrána, J.; Dundálek, J.; Kosek, J. Performance evaluation of thermally treated graphite felt electrodes for vanadium redox flow battery and their four-point single cell characterization. *J. Power Sources* **2018**, *380*, 105–114. [[CrossRef](#)]
141. Melke, J.; Jakes, P.; Langner, J.; Riekehr, L.; Kunz, U.; Zhao-Karger, Z.; Nefedov, A.; Sezen, H.; Wöll, C.; Ehrenberg, H. Carbon materials for the positive electrode in all-vanadium redox flow batteries. *Carbon* **2014**, *78*, 220–230. [[CrossRef](#)]
142. Bourke, A.; Miller, M.; Lynch, R.P.; Wainright, J.; Savinell, R.; Buckley, D. Effect of cathodic and anodic treatments of carbon on the electrode kinetics of VIV/VV oxidation-reduction. *J. Electrochem. Soc.* **2015**, *162*, A1547. [[CrossRef](#)]
143. Gao, C.; Wang, N.; Peng, S.; Liu, S.; Lei, Y.; Liang, X.; Zeng, S.; Zi, H. Influence of Fenton's reagent treatment on electrochemical properties of graphite felt for all vanadium redox flow battery. *Electrochim. Acta* **2013**, *88*, 193–202. [[CrossRef](#)]
144. Flox, C.; Skoumal, M.; Rubio-Garcia, J.; Andreu, T.; Morante, J.R. Strategies for enhancing electrochemical activity of carbon-based electrodes for all-vanadium redox flow batteries. *Appl. Energy* **2013**, *109*, 344–351. [[CrossRef](#)]
145. Li, X.-G.; Huang, K.-L.; Liu, S.-Q.; Tan, N.; Chen, L.-Q. Characteristics of graphite felt electrode electrochemically oxidized for vanadium redox battery application. *Trans. Nonferrous Met. Soc. China* **2007**, *17*, 195–199. [[CrossRef](#)]
146. Zhong, S.; Padeste, C.; Kazacos, M.; Skyllas-Kazacos, M. Comparison of the physical, chemical and electrochemical properties of rayon-and polyacrylonitrile-based graphite felt electrodes. *J. Power Sources* **1993**, *45*, 29–41. [[CrossRef](#)]
147. Friedl, J.; Bauer, C.M.; Rinaldi, A.; Stimming, U. Electron transfer kinetics of the VO₂₊/VO₂₊–Reaction on multi-walled carbon nanotubes. *Carbon* **2013**, *63*, 228–239. [[CrossRef](#)]
148. IRENA. *Electricity Storage and Renewables: Costs and Markets to 2030*; International Renewable Energy Agency: Abu Dhabi, United Arab Emirates, 2017.
149. Zou, W.-J.; Kim, Y.-B.; Jung, S. Capacity fade prediction for vanadium redox flow batteries during long-term operations. *Appl. Energy* **2024**, *356*, 122329. [[CrossRef](#)]
150. Khaki, B.; Das, P. Definition of multi-objective operation optimization of vanadium redox flow and lithium-ion batteries considering levelized cost of energy, fast charging, and energy efficiency based on current density. *J. Energy Storage* **2023**, *64*, 107246. [[CrossRef](#)]
151. Uhrig, M.; Koenig, S.; Suriyah, M.R.; Leibfried, T. Lithium-based vs. Vanadium Redox Flow Batteries—A Comparison for Home Storage Systems. *Energy Procedia* **2016**, *99*, 35–43. [[CrossRef](#)]
152. Kim, S.; Vijayakumar, M.; Wang, W.; Zhang, J.; Chen, B.; Nie, Z.; Chen, F.; Hu, J.; Li, L.; Yang, Z. Chloride supporting electrolytes for all-vanadium redox flow batteries. *Phys. Chem. Chem. Phys.* **2011**, *13*, 18186–18193. [[CrossRef](#)]
153. Tolmachev, Y.V. Review—Flow Batteries from 1879 to 2022 and Beyond. *J. Electrochem. Soc.* **2023**, *170*, 030505. [[CrossRef](#)]
154. Puleston, T.; Serra, M.; Costa-Castelló, R. Vanadium redox flow battery capacity loss mitigation strategy based on a comprehensive analysis of electrolyte imbalance effects. *Appl. Energy* **2024**, *355*, 122271. [[CrossRef](#)]
155. Huang, Z.; Liu, Y.; Xie, X.; Huang, C.; Huang, Q.; Guo, Z.; Liu, Y. Experimental Validation of Side Reaction on Capacity Fade of Vanadium Redox Flow Battery. *J. Electrochem. Soc.* **2024**, *171*, 010521. [[CrossRef](#)]
156. Trovò, A.; Rugna, M.; Poli, N.; Guarneri, M. Prospects for industrial vanadium flow batteries. *Ceram. Int.* **2023**, *49*, 24487–24498. [[CrossRef](#)]
157. Dieterle, M.; Fischer, P.; Pons, M.-N.; Blume, N.; Minke, C.; Bischi, A. Life cycle assessment (LCA) for flow batteries: A review of methodological decisions. *Sustain. Energy Technol. Assess.* **2022**, *53*, 102457. [[CrossRef](#)]
158. H2 Inc. Recent Projects, 2022. Available online: http://www.h2aec.com/eng/news_view.do (accessed on 31 October 2022).
159. Sun, C.; Zhang, H. Review of the Development of First-Generation Redox Flow Batteries: Iron-Chromium System. *ChemSusChem* **2022**, *15*, e202101798. [[CrossRef](#)] [[PubMed](#)]

160. Codina, G.; Perez, J.R.; Lopez-Atalaya, M.; Vasquez, J.L.; Aldaz, A. Development of a 0.1 kW power accumulation pilot plant based on an Fe/Cr redox flow battery Part I. Considerations on flow-distribution design. *J. Power Sources* **1994**, *48*, 293–302. [[CrossRef](#)]
161. Lopez-Atalaya, M.; Codina, G.; Perez, J.R.; Vazquez, J.L.; Aldaz, A. Optimization studies on a Fe/Cr redox flow battery. *J. Power Sources* **1992**, *39*, 147–154. [[CrossRef](#)]
162. Hagedorn, N.H. *NASA Redox Storage System Development Project Final Report*; NASA: Washington, DC, USA, 1984.
163. Shimada, M.; Tsuzuki, Y.; Iizuka, Y.; Inoue, M. Investigation of the aqueous Fe-Cr redox flow cell. *Chem. Ind.* **1988**, *80*–82.
164. Wu, M.; Nan, M.; Ye, Y.; Yang, M.; Qiao, L.; Zhang, H.; Ma, X. A highly active electrolyte for high-capacity iron-chromium flow batteries. *Appl. Energy* **2024**, *358*, 122534. [[CrossRef](#)]
165. Wan, C.T.-C.; Rodby, K.E.; Perry, M.L.; Chiang, Y.-M.; Brushett, F.R. Hydrogen evolution mitigation in iron-chromium redox flow batteries via electrochemical purification of the electrolyte. *J. Power Sources* **2023**, *554*, 232248. [[CrossRef](#)]
166. Krown, C.M. State of Charge (SoC) of the Vanadium and Other Redox Flow Batteries: Identification of the Electrode and Bipolar Plate Contributions. *J. Electrochem. Soc.* **2024**, *171*, 100523. [[CrossRef](#)]
167. Mans, N.; Krieg, H.M.; van der Westhuizen, D.J. The Effect of Electrolyte Composition on the Performance of a Single-Cell Iron-Chromium Flow Battery. *Adv. Energy Sustain. Res.* **2023**, *5*, 2300238. [[CrossRef](#)]
168. Johnson, D.A.; Reid, M.A. Chemical and Electrochemical Behavior of the Cr(III)/Cr(II) Half-Cell in the Iron-Chromium Redox Energy Storage System. *J. Electrochem. Soc.* **1985**, *132*, 1058–1062. [[CrossRef](#)]
169. Niu, Y.; Guo, C.; Liu, Y.; Wu, G.; Zhou, T.; Qu, F.; Yang, Z.; Heydari, A.; Xu, C.; Xu, Q. Fabrication of highly effective electrodes for iron chromium redox flow battery. *Nano Res.* **2023**, *17*, 3988–3996. [[CrossRef](#)]
170. Chen, N.; Zhang, H.; Luo, X.-D.; Sun, C.-Y. SiO₂-decorated graphite felt electrode by silicic acid etching for iron-chromium redox flow battery. *Electrochim. Acta* **2020**, *336*, 135646. [[CrossRef](#)]
171. Li, Z.; Guo, L.; Chen, N.; Su, Y.; Wang, X. Boric acid thermal etching graphite felt as a high-performance electrode for iron-chromium redox flow battery. *Mater. Res. Express* **2022**, *9*, 025601. [[CrossRef](#)]
172. Zhang, H.; Chen, N.; Sun, C.; Luo, X. Investigations on physicochemical properties and electrochemical performance of graphite felt and carbon felt for iron-chromium redox flow battery. *Int. J. Energy Res.* **2020**, *44*, 3839–3853. [[CrossRef](#)]
173. Su, Y.; Chen, N.; Ren, H.-L.; Li, C.-W.; Guo, L.-L.; Li, Z.; Wang, X.-M. Application of modified graphite felt as electrode material: A review. *Carbon Lett.* **2023**, *33*, 1–16. [[CrossRef](#)]
174. Wang, S.; Xu, Z.; Wu, X.; Zhao, H.; Zhao, J.; Liu, J.; Yan, C.; Fan, X. Analyses and optimization of electrolyte concentration on the electrochemical performance of iron-chromium flow battery. *Appl. Energy* **2020**, *271*, 115252. [[CrossRef](#)]
175. Liu, W.; Lu, W.; Zhang, H.; Li, X. Aqueous Flow Batteries: Research and Development. *Chemistry* **2019**, *25*, 1649–1664. [[CrossRef](#)]
176. Zhang, S.; Guo, W.; Yang, F.; Zheng, P.; Qiao, R.; Li, Z. Recent Progress in Polysulfide Redox-Flow Batteries. *Batter. Supercaps* **2019**, *2*, 627–637. [[CrossRef](#)]
177. Lu, G.; Wang, Z.; Zhang, S.; Ding, J.; Luo, J.; Liu, X. Cathode materials for halide-based aqueous redox flow batteries: Recent progress and future perspectives. *Nanoscale* **2023**, *15*, 4250–4260. [[CrossRef](#)]
178. Khan, I.A.; Alzahrani, A.S.; Ali, S.; Mansha, M.; Tahir, M.N.; Khan, M.; Qayyum, H.A.; Khan, S.A. Development of Membranes and Separators to Inhibit Cross-Shuttling of Sulfur in Polysulfide-Based Redox Flow Batteries: A Review. *Chem Rec* **2024**, *24*, e202300171. [[CrossRef](#)]
179. Qu, C.; Chen, Y.; Yang, X.; Zhang, H.; Li, X.; Zhang, H. LiNO₃-free electrolyte for Li-S battery: A solvent of choice with low K_{sp} of polysulfide and low dendrite of lithium. *Nano Energy* **2017**, *39*, 262–272. [[CrossRef](#)]
180. Pan, H.; Wei, X.; Henderson, W.A.; Shao, Y.; Chen, J.; Bhattacharya, P.; Xiao, J.; Liu, J. On the Way Toward Understanding Solution Chemistry of Lithium Polysulfides for High Energy Li-S Redox Flow Batteries. *Adv. Energy Mater.* **2015**, *5*, 1500113. [[CrossRef](#)]
181. Yamin, H.; Gorenstein, A.; Penciner, J.; Sternberg, Y.; Peled, E. Lithium sulfur battery: Oxidation/reduction mechanisms of polysulfides in THF solutions. *J. Electrochem. Soc.* **1988**, *135*, 1045. [[CrossRef](#)]
182. Fan, F.Y.; Chiang, Y.-M. Electrodeposition Kinetics in Li-S Batteries: Effects of Low Electrolyte/Sulfur Ratios and Deposition Surface Composition. *J. Electrochem. Soc.* **2017**, *164*, A917–A922. [[CrossRef](#)]
183. Duduta, M.; Ho, B.; Wood, V.C.; Limthongkul, P.; Brunini, V.E.; Carter, W.C.; Chiang, Y.-M. Semi-Solid Lithium Rechargeable Flow Battery. *Adv. Energy Mater.* **2011**, *1*, 511–516. [[CrossRef](#)]
184. Yang, F.; Mousavie, S.M.A.; Oh, T.K.; Yang, T.; Lu, Y.; Farley, C.; Bodnar, R.J.; Niu, L.; Qiao, R.; Li, Z. Sodium-Sulfur Flow Battery for Low-Cost Electrical Storage. *Adv. Energy Mater.* **2018**, *8*, 1701991. [[CrossRef](#)]
185. Li, Z.; Pan, M.S.; Su, L.; Tsai, P.-C.; Badel, A.F.; Valle, J.M.; Eiler, S.L.; Xiang, K.; Brushett, F.R.; Chiang, Y.-M. Air-Breathing Aqueous Sulfur Flow Battery for Ultralow-Cost Long-Duration Electrical Storage. *Joule* **2017**, *1*, 306–327. [[CrossRef](#)]
186. Zhang, C.; Yuan, Z.; Li, X. Designing Better Flow Batteries: An Overview on Fifty Years' Research. *ACS Energy Lett.* **2024**, *9*, 3456–3473. [[CrossRef](#)]

187. Petrov, M.M.; Modestov, A.D.; Konev, D.V.; Antipov, A.E.; Loktionov, P.A.; Pichugov, R.D.; Kartashova, N.V.; Glazkov, A.T.; Abunaeva, L.Z.; Andreev, V.N. Redox flow batteries: Role in modern electric power industry and comparative characteristics of the main types. *Russ. Chem. Rev.* **2021**, *90*, 677. [[CrossRef](#)]
188. Li, Z.; Weng, G.; Zou, Q.; Cong, G.; Lu, Y.-C. A high-energy and low-cost polysulfide/iodide redox flow battery. *Nano Energy* **2016**, *30*, 283–292. [[CrossRef](#)]
189. Leung, P.; Shah, A.A.; Sanz, L.; Flox, C.; Morante, J.; Xu, Q.; Mohamed, M.; De León, C.P.; Walsh, F. Recent developments in organic redox flow batteries: A critical review. *J. Power Sources* **2017**, *360*, 243–283. [[CrossRef](#)]
190. Cao, J.; Tian, J.; Xu, J.; Wang, Y. Organic Flow Batteries: Recent Progress and Perspectives. *Energy Fuels* **2020**, *34*, 13384–13411. [[CrossRef](#)]
191. Quan, M.; Sanchez, D.; Wasylkiw, M.F.; Smith, D.K. Voltammetry of quinones in unbuffered aqueous solution: Reassessing the roles of proton transfer and hydrogen bonding in the aqueous electrochemistry of quinones. *J. Am. Chem. Soc.* **2007**, *129*, 12847–12856. [[CrossRef](#)] [[PubMed](#)]
192. Krishnamurti, V.; Yang, B.; Murali, A.; Patil, S.; Prakash, G.K.S.; Narayan, S. Aqueous organic flow batteries for sustainable energy storage. *Curr. Opin. Electrochem.* **2022**, *35*, 101100. [[CrossRef](#)]
193. Yang, G.; Zhu, Y.; Hao, Z.; Lu, Y.; Zhao, Q.; Zhang, K.; Chen, J. Organic Electroactive Materials for Aqueous Redox Flow Batteries. *Adv Mater* **2023**, *35*, e2301898. [[CrossRef](#)] [[PubMed](#)]
194. Orita, A.; Verde, M.G.; Sakai, M.; Meng, Y.S. A biomimetic redox flow battery based on flavin mononucleotide. *Nat. Commun.* **2016**, *7*, 13230. [[CrossRef](#)] [[PubMed](#)]
195. Ji, Y.; Goulet, M.A.; Pollack, D.A.; Kwabi, D.G.; Jin, S.; De Porcellinis, D.; Kerr, E.F.; Gordon, R.G.; Aziz, M.J. A phosphonate-functionalized quinone redox flow battery at near-neutral pH with record capacity retention rate. *Adv. Energy Mater.* **2019**, *9*, 1900039. [[CrossRef](#)]
196. Khataee, A.; Wedege, K.; Dražević, E.; Bentien, A. Differential pH as a method for increasing cell potential in organic aqueous flow batteries. *J. Mater. Chem. A* **2017**, *5*, 21875–21882. [[CrossRef](#)]
197. Lin, K.; Chen, Q.; Gerhardt, M.R.; Tong, L.; Kim, S.B.; Eisenach, L.; Valle, A.W.; Hardee, D.; Gordon, R.G.; Aziz, M.J. Alkaline quinone flow battery. *Science* **2015**, *349*, 1529–1532. [[CrossRef](#)]
198. Goulet, M.-A.; Tong, L.; Pollack, D.A.; Tabor, D.P.; Odom, S.A.; Aspuru-Guzik, A.; Kwan, E.E.; Gordon, R.G.; Aziz, M.J. Extending the lifetime of organic flow batteries via redox state management. *J. Am. Chem. Soc.* **2019**, *141*, 8014–8019. [[CrossRef](#)]
199. Darling, R.; Gallagher, K.; Xie, W.; Su, L.; Brushett, F. Transport property requirements for flow battery separators. *J. Electrochem. Soc.* **2015**, *163*, A5029. [[CrossRef](#)]
200. Bradley, C.S. Secondary Battery. US Patent 312,802, 24 February 1885.
201. Singh, P. Application of non-aqueous solvents to batteries. *J. Power Sources* **1984**, *11*, 135–142. [[CrossRef](#)]
202. Bloch, R.; Farkas, L.; Schnerb, J.; Winograd, F. On the Phase Diagram of the Two-Component System Bromine-Tetramethylammonium Bromide and the Solubilities of the Components in Water. *J. Phys. Chem.* **1949**, *53*, 1117–1125. [[CrossRef](#)]
203. Kordesch, K.V.; Fabjan, C.; Daniel-Ivad, J.; Oliveira, J. Rechargeable zinc-carbon hybrid cells. *J. Power Sources* **1997**, *65*, 77–80. [[CrossRef](#)]
204. Choi, G.; Sullivan, P.; Lv, X.L.; Li, W.; Lee, K.; Kong, H.; Gessler, S.; Schmidt, J.R.; Feng, D. Soft-hard zwitterionic additives for aqueous halide flow batteries. *Nature* **2024**, *635*, 89–95. [[CrossRef](#)]
205. Khor, A.; Leung, P.; Mohamed, M.R.; Flox, C.; Xu, Q.; An, L.; Wills, R.G.A.; Morante, J.R.; Shah, A.A. Review of zinc-based hybrid flow batteries: From fundamentals to applications. *Mater. Today Energy* **2018**, *8*, 80–108. [[CrossRef](#)]
206. Yuan, Z.; Liu, X.; Xu, W.; Duan, Y.; Zhang, H.; Li, X. Negatively charged nanoporous membrane for a dendrite-free alkaline zinc-based flow battery with long cycle life. *Nat. Commun.* **2018**, *9*, 3731. [[CrossRef](#)]
207. Liu, X.; Zhang, H.; Duan, Y.; Yuan, Z.; Li, X. Effect of electrolyte additives on the water transfer behavior for alkaline zinc–iron flow batteries. *ACS Appl. Mater. Interfaces* **2020**, *12*, 51573–51580. [[CrossRef](#)]
208. Yuan, Z.; Duan, Y.; Liu, T.; Zhang, H.; Li, X. Toward a low-cost alkaline zinc–iron flow battery with a polybenzimidazole custom membrane for stationary energy storage. *iScience* **2018**, *3*, 40–49. [[CrossRef](#)]
209. Fell, E.M.; De Porcellinis, D.; Jing, Y.; Gutierrez-Venegas, V.; George, T.Y.; Gordon, R.G.; Granados-Focil, S.; Aziz, M.J. Long-term stability of ferri-/ferrocyanide as an electroactive component for redox flow battery applications: On the origin of apparent capacity fade. *J. Electrochem. Soc.* **2023**, *170*, 070525. [[CrossRef](#)]
210. Zhi, L.; Liao, C.; Xu, P.; Sun, F.; Fan, F.; Li, G.; Yuan, Z.; Li, X. New Alkaliescent Electrolyte Chemistry for Zinc-Ferricyanide Flow Battery. *Angew. Chem. Int. Ed.* **2024**, *63*, e202403607. [[CrossRef](#)]
211. Lee, J.-i.; Faheem, A.B.; Jang, W.J.; Kim, K.; Cha, J.S.; Seo, N.-U.; Kim, H.; Lee, K.-K.; Yang, J.H. Effective Enhancement of Energy Density of Zinc-Polyiodide Flow Batteries by Organic/Penta-iodide Complexation. *ACS Appl. Mater. Interfaces* **2023**, *15*, 48122–48134. [[CrossRef](#)] [[PubMed](#)]

212. Wang, M.; Zheng, X.; Cui, Y.; Chen, W. Aqueous Electrolytic Zinc-Manganese Dioxide Batteries. In *Aqueous Zinc Batteries*; World Scientific: Singapore, 2024; pp. 139–175.
213. Liu, Y.; Xie, C.; Li, X. Bromine assisted MnO_2 dissolution chemistry: Toward a hybrid flow battery with energy density of over 300 Wh L^{-1} . *Angew. Chem.* **2022**, *134*, e202213751. [CrossRef]
214. Winsberg, J.; Janoschka, T.; Morgenstern, S.; Hagemann, T.; Muench, S.; Hauffman, G.; Gohy, J.F.; Hager, M.D.; Schubert, U.S. Poly (TEMPO)/zinc hybrid-flow battery: A novel, “green,” high voltage, and safe energy storage system. *Adv. Mater.* **2016**, *28*, 2238–2243. [CrossRef] [PubMed]
215. Arenas, L.F.; Walsh, F.C.; de León, C.P. Zinc–Cerium and Related Cerium-Based Flow Batteries: Progress and Challenges. *Flow Batter. Fundam. Appl.* **2023**, *2*, 819–835.
216. Hruska, L.W.; Savinell, R.F. Investigation of factors affecting performance of the iron-redox battery. *J. Electrochem. Soc.* **1981**, *128*, 18. [CrossRef]
217. Hawthorne, K.L.; Petek, T.J.; Miller, M.A.; Wainright, J.S.; Savinell, R.F. An Investigation into Factors Affecting the Iron Plating Reaction for an All-Iron Flow Battery. *J. Electrochem. Soc.* **2015**, *162*, A108–A113. [CrossRef]
218. Belongia, S.; Wang, X.; Zhang, X. Progresses and Perspectives of All-Iron Aqueous Redox Flow Batteries. *Adv. Funct. Mater.* **2024**, *34*, 2302077. [CrossRef]
219. Dinesh, A.; Olivera, S.; Venkatesh, K.; Santosh, M.S.; Priya, M.G.; Inamuddin; Asiri, A.M.; Muralidhara, H.B. Iron-based flow batteries to store renewable energies. *Environ. Chem. Lett.* **2018**, *16*, 683–694. [CrossRef]
220. Zhang, H.; Sun, C. Cost-effective iron-based aqueous redox flow batteries for large-scale energy storage application: A review. *J. Power Sources* **2021**, *493*, 229445. [CrossRef]
221. Hawthorne, K.L.; Wainright, J.S.; Savinell, R.F. Studies of Iron-Ligand Complexes for an All-Iron Flow Battery Application. *J. Electrochem. Soc.* **2014**, *161*, A1662–A1671. [CrossRef]
222. Hawthorne, K.; Wainright, J.; Savinell, R. Electrokinetic Studies of Iron-Ligand Complexes for An All-Iron Redox Flow Battery Application. *Meet. Abstr.* **2013**, MA2013–02, 297. [CrossRef]
223. Ebner, S.; Spirk, S.; Stern, T.; Mair-Bauernfeind, C. How green are redox flow batteries? *ChemSusChem* **2023**, *16*, e202201818. [CrossRef] [PubMed]
224. Gao, J.; Amini, K.; George, T.Y.; Jing, Y.; Tsukamoto, T.; Xi, D.; Gordon, R.G.; Aziz, M.J. A high potential, low capacity fade rate iron complex posolyte for aqueous organic flow batteries. *Adv. Energy Mater.* **2022**, *12*, 2202444. [CrossRef]
225. Song, Y.; Zhang, K.; Li, X.; Yan, C.; Liu, Q.; Tang, A. Tuning the ferrous coordination structure enables a highly reversible Fe anode for long-life all-iron flow batteries. *J. Mater. Chem. A* **2021**, *9*, 26354–26361. [CrossRef]
226. Helwig, A.; Bell, J. What energy storage technologies will Australia need as renewable energy penetration rises? *J. Energy Storage* **2024**, *95*, 112701.
227. Stocks, M.; Stocks, R.; Lu, B.; Cheng, C.; Blakers, A. Global atlas of closed-loop pumped hydro energy storage. *Joule* **2021**, *5*, 270–284. [CrossRef]
228. ARENA. Hydropower/Pumped Hydro Energy Storage. 2024. Available online: <https://arena.gov.au/renewable-energy/pumped-hydro-energy-storage/> (accessed on 20 November 2024).
229. Tong, W.; Lu, Z.; Sun, J.; Zhao, G.; Han, M.; Xu, J. Solid gravity energy storage technology: Classification and comparison. *Energy Rep.* **2022**, *8*, 926–934. [CrossRef]
230. Hill, J. *Australian Start-Up Secures \$9m for Mine-Based Gravity Energy Storage Technology*; Renewable economy: Mullumbimby, Australia, 2024.
231. Bai, H.; Song, Z. Lithium-ion battery; sodium-ion battery, or redox-flow battery: A comprehensive comparison in renewable energy systems. *J. Power Sources* **2023**, *580*, 233426. [CrossRef]
232. Wanner, M. Transformation of electrical energy into hydrogen and its storage. *Eur. Phys. J. Plus* **2021**, *136*, 593. [CrossRef]
233. DCCEEW. *State of Hydrogen*; Australian Government: Canberra, Australia, 2022.
234. ARENA. What Is Hydrogen Energy? 2024. Available online: <https://arena.gov.au/renewable-energy/hydrogen/> (accessed on 11 November 2024).
235. Dutta, A.; Mitra, S.; Basak, M.; Banerjee, T. A comprehensive review on batteries and supercapacitors: Development and challenges since their inception. *Energy Storage* **2023**, *5*, e339. [CrossRef]
236. Dănilă, E.; Lucache, D.D. History of the first energy storage systems. In Proceedings of the Paper Delivered at the 3rd International Symposium on the History of Electrical Engineering and of Tertiary-Level Engineering Education, Iași, Romania, 27–29 October 2010.
237. Russell, C.A. The electrochemical theory of sir Humphry Davy: Part I: The voltaic pile and electrolysis. In *From Atoms to Molecules*; Routledge: London, UK, 2024; pp. 23–35.
238. Hur, J.I.; Smith, L.C.; Dunn, B. High areal energy density 3D lithium-ion microbatteries. *Joule* **2018**, *2*, 1187–1201. [CrossRef]
239. Ha-Duong, M. Battery Electricity Storage Systems, the energy sector’s next big tech. *Tia Sáng* **2024**, hal-04650083. Available online: <https://hal.science/hal-04650083v1> (accessed on 9 November 2023).

240. Degen, F.; Winter, M.; Bendig, D.; Tübke, J. Energy consumption of current and future production of lithium-ion and post lithium-ion battery cells. *Nat. Energy* **2023**, *8*, 1284–1295. [CrossRef]
241. Zalosh, R.; Gandhi, P.; Barowy, A. Lithium-ion energy storage battery explosion incidents. *J. Loss Prev. Process Ind.* **2021**, *72*, 104560. [CrossRef]
242. SARET. *Lithium Ion Battery Incidents* 2024; Fire and Rescue Services New South Wales: Greenacre, Australia, 2024.
243. Ruether, T. Lithium-Ion Battery Recyclin. 2024. Available online: <https://www.csiro.au/en/research/technology-space/energy/energy-in-the-circular-economy/battery-recycling> (accessed on 20 November 2024).
244. Roberts, D.; Brown, S. The economics of firm solar power from Li-ion and vanadium flow batteries in California. *MRS Energy Sustain.* **2022**, *9*, 129–141. [CrossRef]
245. Trovò, A.; Marini, G.; Zamboni, W.; Sessa, S.D. Redox Flow Batteries: A Glance at Safety and Regulation Issues. *Electronics* **2023**, *12*, 1844. [CrossRef]
246. Chen, T.; Jin, Y.; Lv, H.; Yang, A.; Liu, M.; Chen, B.; Xie, Y.; Chen, Q. Applications of Lithium-Ion Batteries in Grid-Scale Energy Storage Systems. *Trans. Tianjin Univ.* **2020**, *26*, 208–217. [CrossRef]
247. Escobar-Hernandez, H.U.; Gustafson, R.M.; Papadaki, M.I.; Sachdeva, S.; Mannan, M.S. Thermal Runaway in Lithium-Ion Batteries: Incidents, Kinetics of the Runaway and Assessment of Factors Affecting Its Initiation. *J. Electrochem. Soc.* **2016**, *163*, A2691–A2701. [CrossRef]
248. Sun, J.; Li, J.; Zhou, T.; Yang, K.; Wei, S.; Tang, N.; Dang, N.; Li, H.; Qiu, X.; Chen, L. Toxicity, a serious concern of thermal runaway from commercial Li-ion battery. *Nano Energy* **2016**, *27*, 313–319. [CrossRef]
249. Peters, J.F.; Baumann, M.; Zimmermann, B.; Braun, J.; Weil, M. The environmental impact of Li-Ion batteries and the role of key parameters—A review. *Renew. Sustain. Energy Rev.* **2017**, *67*, 491–506. [CrossRef]
250. da Silva Lima, L.; Quartier, M.; Buchmayr, A.; Sanjuan-Delmás, D.; Laget, H.; Corbisier, D.; Mertens, J.; Dewulf, J. Life cycle assessment of lithium-ion batteries and vanadium redox flow batteries-based renewable energy storage systems. *Sustain. Energy Technol. Assess.* **2021**, *46*, 101286. [CrossRef]
251. Darling, R.M. Techno-economic analyses of several redox flow batteries using levelized cost of energy storage. *Curr. Opin. Chem. Eng.* **2022**, *37*, 100855. [CrossRef]
252. Vanitec. Map of Vanadium Redox Flow Batteries. 2023. Available online: <https://vanitec.org/vanadium/map> (accessed on 4 February 2025).
253. Australian Department of Climate Change, Energy, the Environment and Water. Renewables. 2023. Available online: <https://www.energy.gov.au/data/renewables> (accessed on 9 November 2023).
254. Thomas, R. *The 82 per Cent National Renewable Energy Target—Where Did It Come from and How Can We Get There?* Australian Energy Council: Canberra, Australia, 2023.
255. Senior, A.; Britt, A.F.; Pheeney, J.; Summerfield, D.; Hughes, A.; Cross, A.; Sexton, M.; Teh, M. *Australia's Identified Mineral Resources 2021*; Department of Industry and Science, Energy and Resources, Geoscience Australia: Canberra, Australia, 2021.
256. Roberts, P. Townsville Vanadium Battery Electrolyte Facility Opens. Manufacturing News 2023. Available online: <https://aumanufacturing.com.au/townsville-vanadium-battery-electrolyte-facility-opens#:~:text=Miner%20and%20manufacturer%20Vecco%20Group,%E2%80%99big%20win%20for%20Queensland%E2%80%99> (accessed on 9 November 2023).
257. Redflow. Redflow Homepage. Available online: <https://redflow.com/> (accessed on 24 April 2024).

Disclaimer/Publisher’s Note: The statements, opinions and data contained in all publications are solely those of the individual author(s) and contributor(s) and not of MDPI and/or the editor(s). MDPI and/or the editor(s) disclaim responsibility for any injury to people or property resulting from any ideas, methods, instructions or products referred to in the content.